



# In search of nc/sc common themes: Working group 3 and 4 joint session





# Objective

I will select aspects of CLIC rf structure work for which I believe are common to both our projects and for which we could potentially establish some kind of joint activities.

I hope that during the discussion we can expand on the list, and find a way to establish some joint activity after the workshop.



We need to cross the grain boundary





# The list

1. rf computation
2. Damping materials
3. Simulation of high-power effects
4. Surface preparation and assembly procedures
5. L-band technology and power sources (covered in next session)

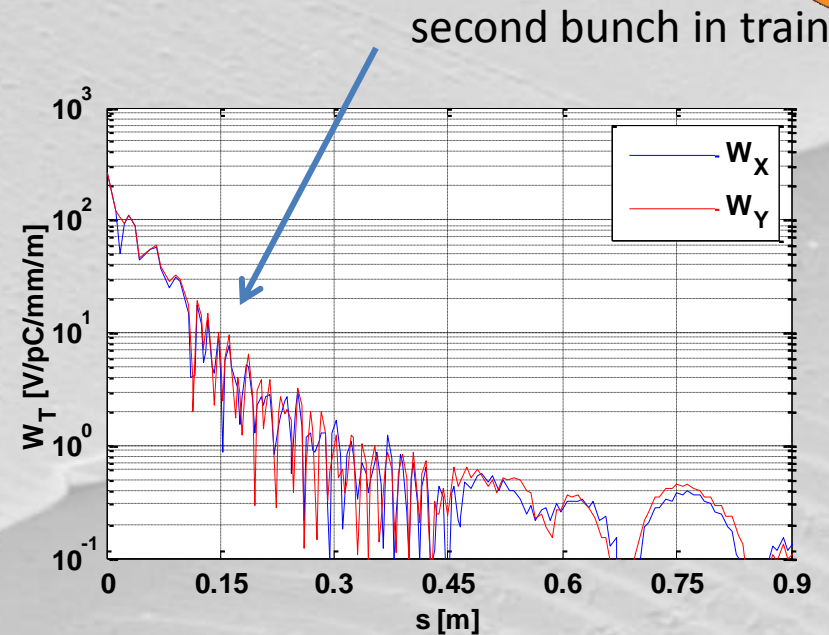
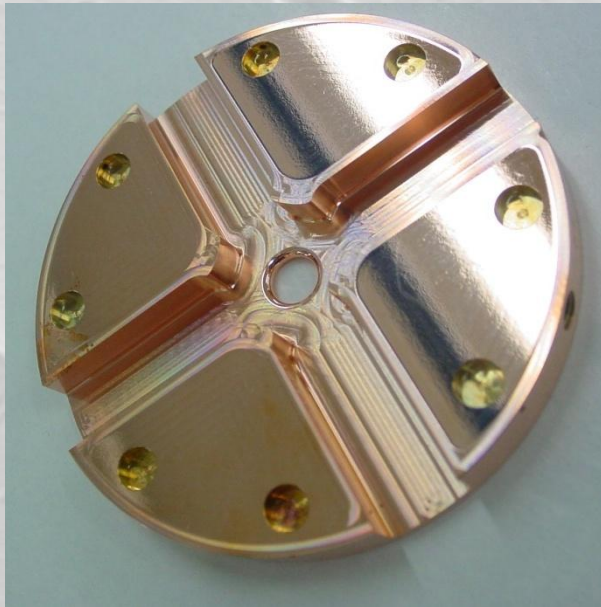




# rf computation

1. HOM suppression
2. linac/rf optimization
3. Advanced computation





Bunches sit at a six fundamental mode bucket separation so the transverse wakefield suppression needs to be very fast. Equivalent Q's are below 10 (some help from detuning) and every cell is “waveguide” damped. We have very strong beam-structure coupling, for efficiency, so the suppression also has to be very deep. Roughly factor 50 by second bunch.



Pursuit of alternatives – potential for better performance or lower cost



# 2.3 Summary of CLIC\_DDS\_C

Dipole mode

Manifold mode

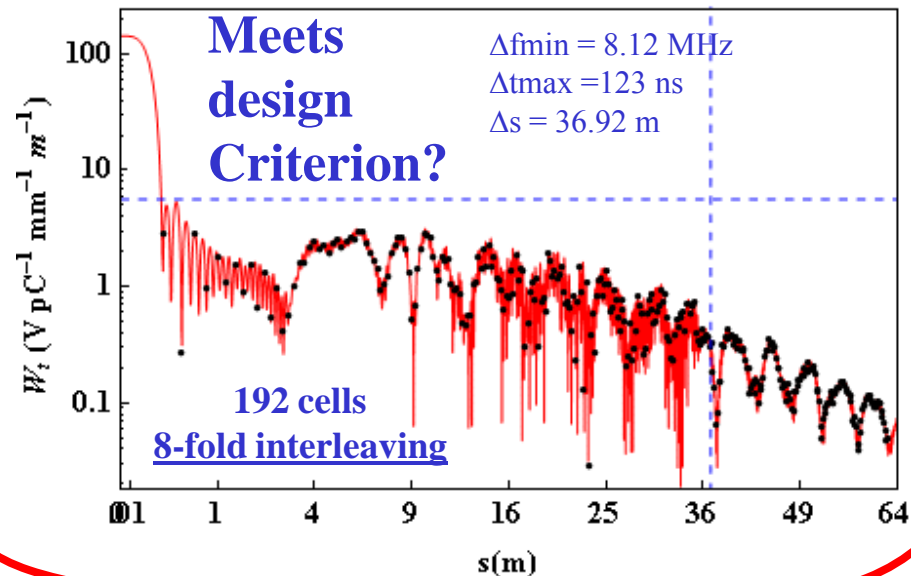
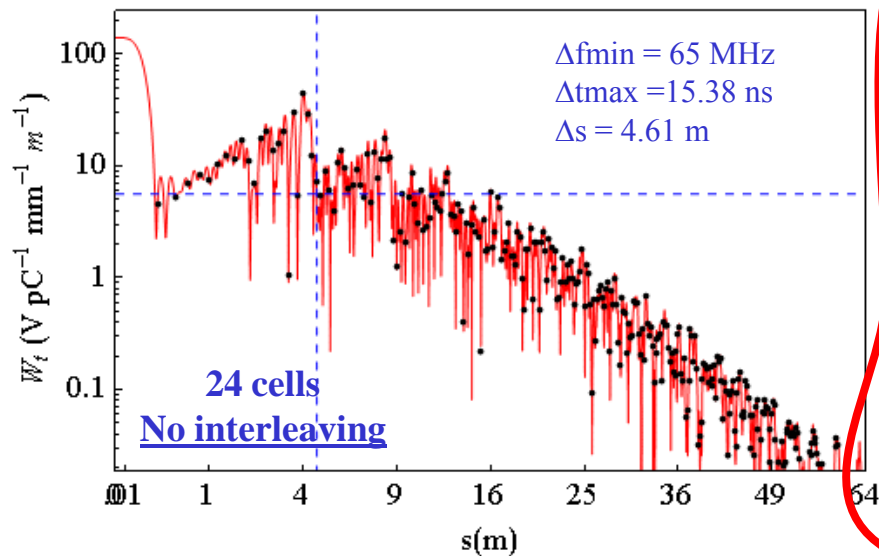
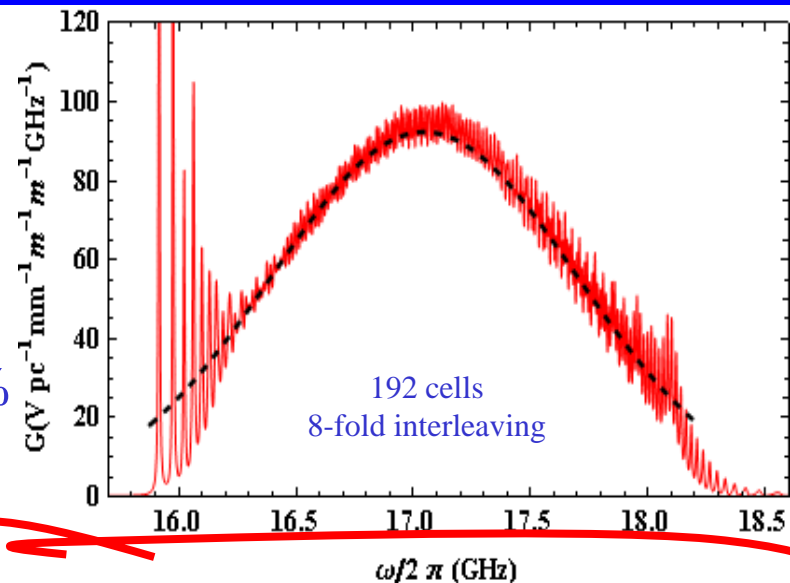
Manifold

Coupling slot

$$\Delta f = 3.6 \sigma$$

$$= 2.3 \text{ GHz}$$

$$\Delta f / f_c = 13.75\%$$

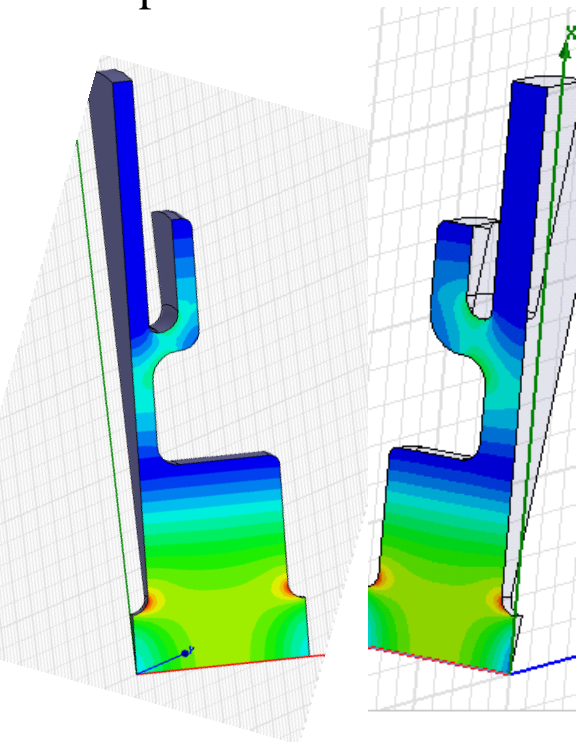




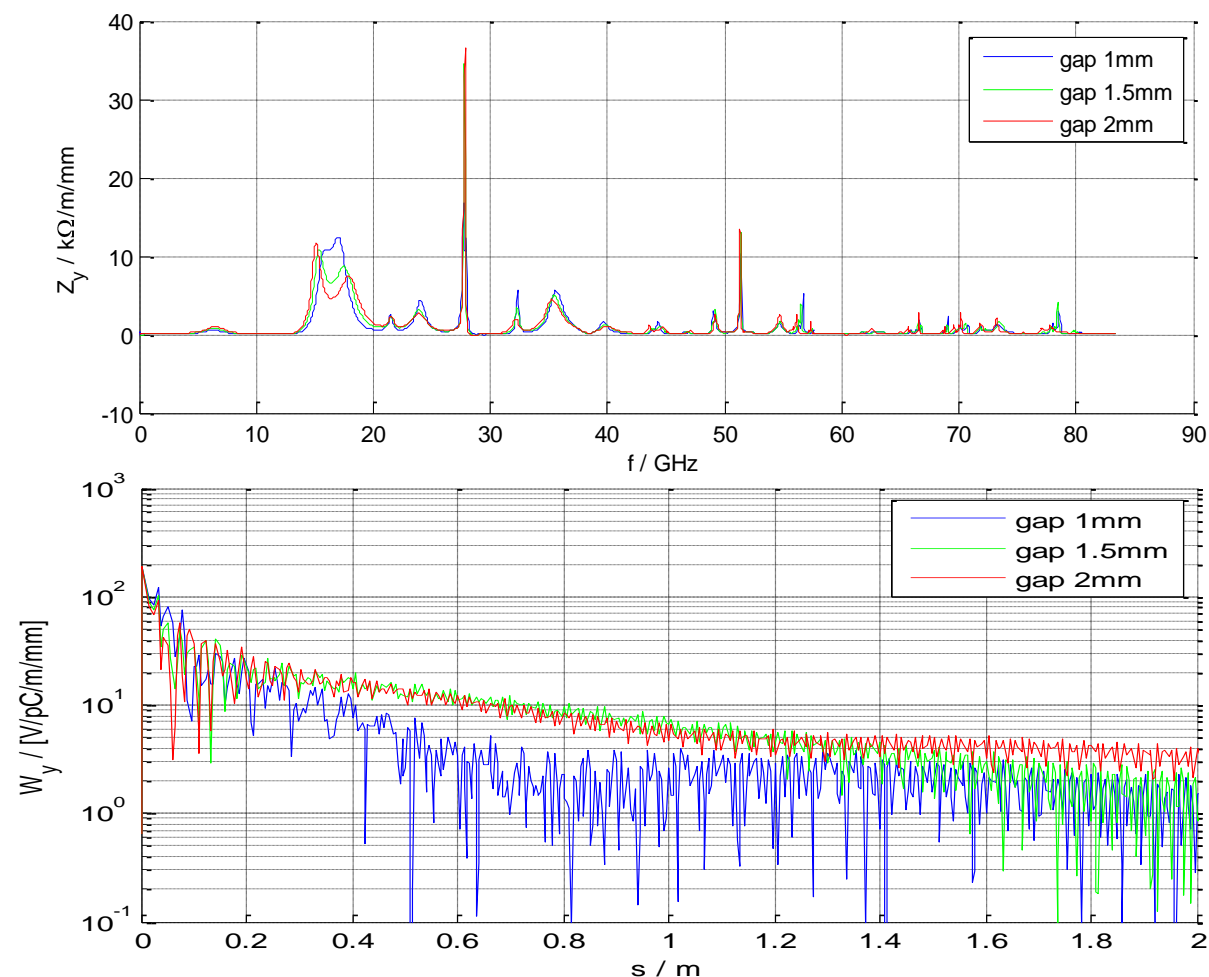
# Wake field simulation with Gdfidl

Gap 1mm

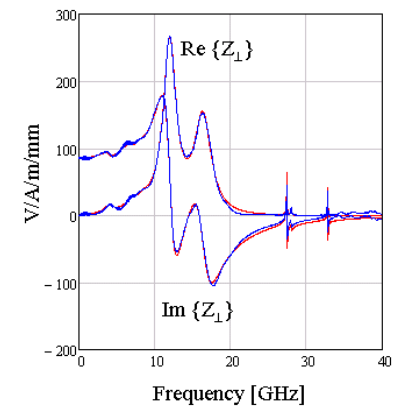
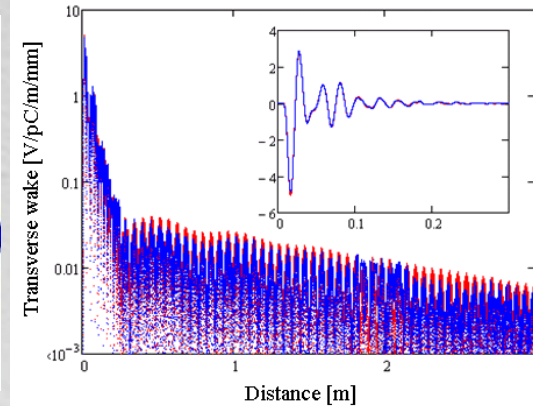
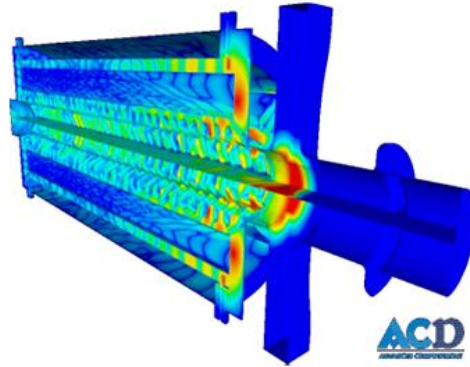
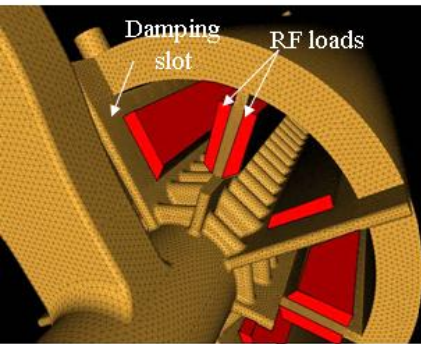
2mm



(Model in HFSS)







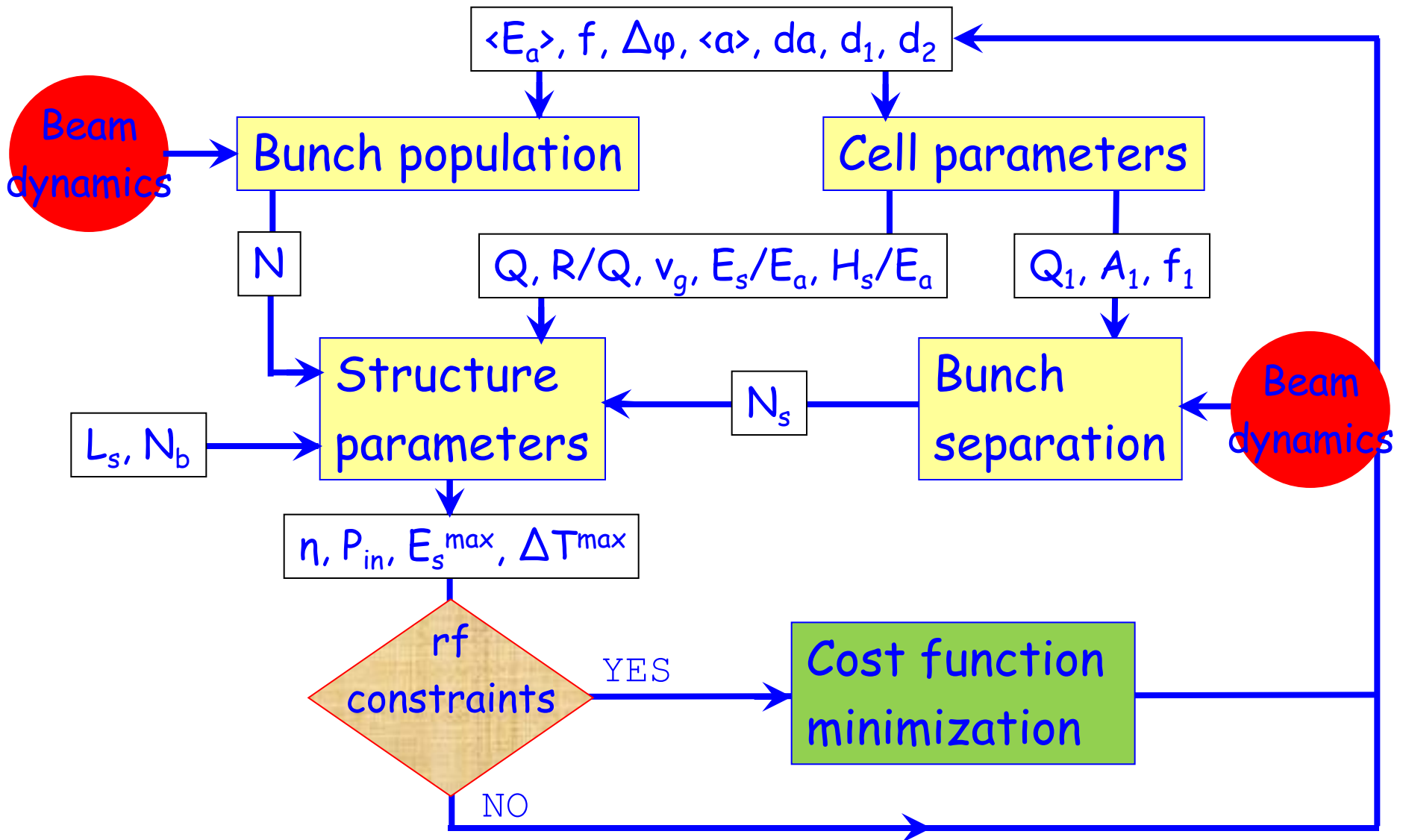
Very low impedance environment ( $a/\lambda=0.46$ ) but bunches sit at every fundamental bucket and the current is 100 A. The drive beam is not a low emittance beam but it is important that instabilities are not amplified by structure resonances – especially when the drive beam is at low energy. Hence specification on effective Q's in HOM spectrum from beam dynamics.

Single bunch transverse wake specification  $< 8$  V/pC/mm/m.

Overmoded structure so transverse wake also at fundamental frequency – damping by symmetry.

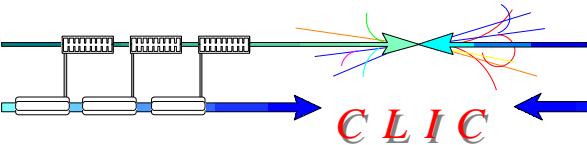


# Optimization procedure

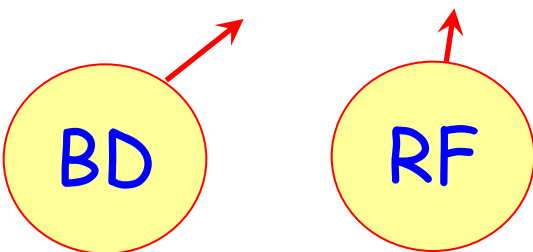




# Beam dynamics input



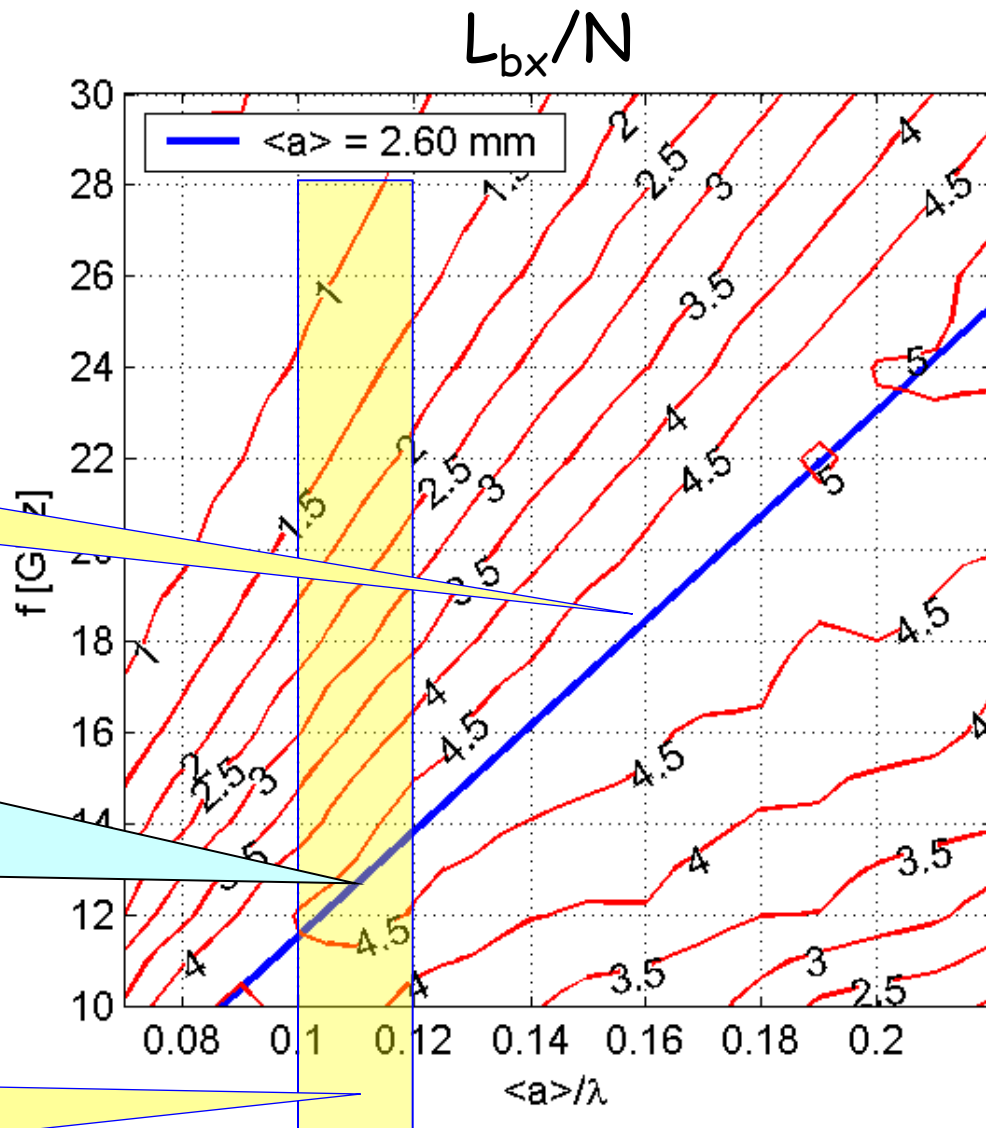
$$FoM = L_{bx} / N \cdot n$$



BD optimum aperture:  
 $\langle a \rangle = 2.6 \text{ mm}$

**Why X-band ?**  
Crossing gives  
optimum frequency

High-power RF optimum  
aperture:  $\langle a \rangle / \lambda = 0.1 \div 0.12$







# Advanced computation



The traditional rf computation tools of the CLIC team have been HFSS and GdfidL and they continue to remain the backbone.

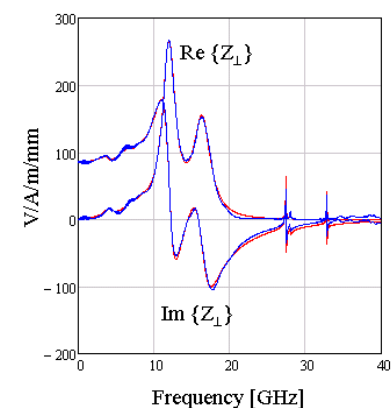
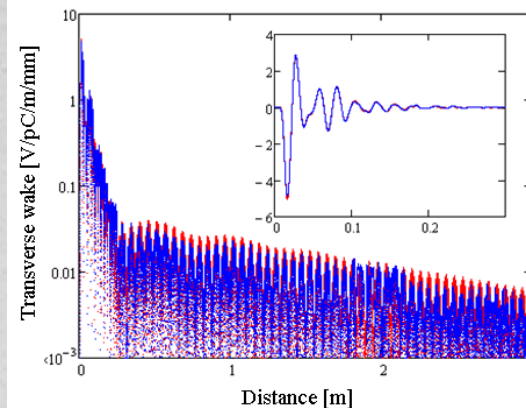
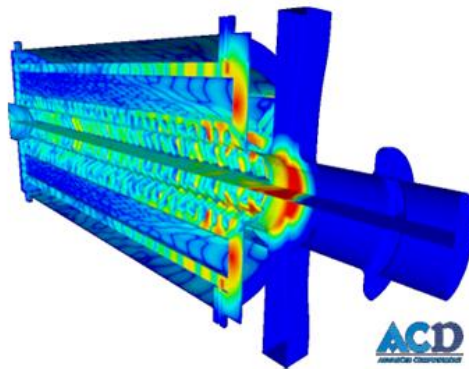
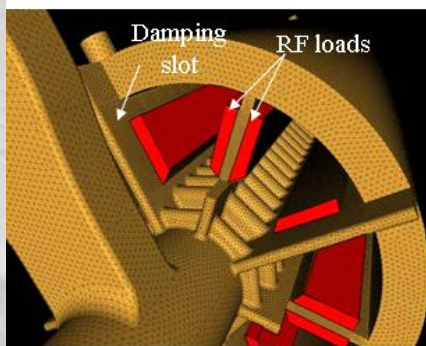
We are now incorporating ACE3P. We do this since it appears to be state-of-the-art accuracy, essential for the really big problems like two-beam acceleration and extendable to issues like breakdown modeling.

People are learning how to use it and we are working through the associated issues – like access to computational time etc.

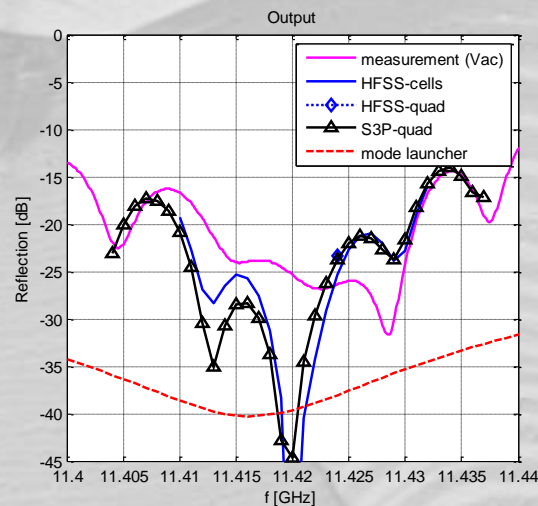
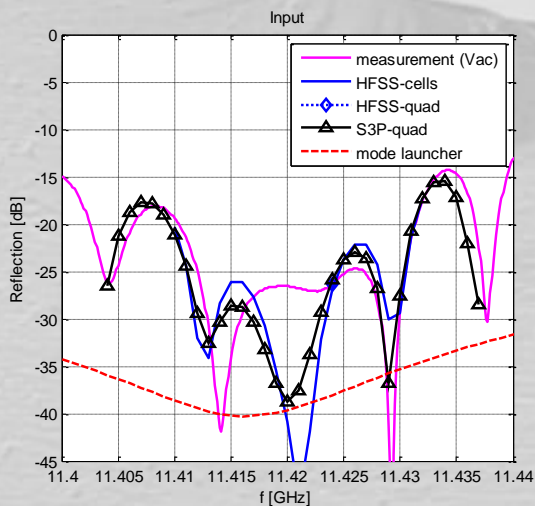
Collaborations are leaders in this activity – SLAC of course but also Oslo University (Eric Adli and Kyrre Sjoebaek) and PSI (Micha Dehler).



# Advanced computation



## GdfidL ACE3P comparison in PETS



## HFSS ACE3P comparison in accelerating structure

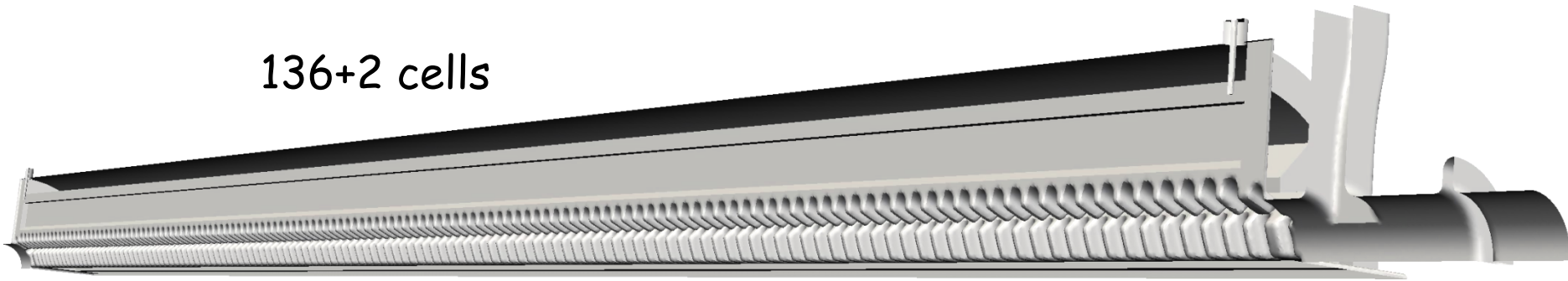


# T3P: Needed for large structures

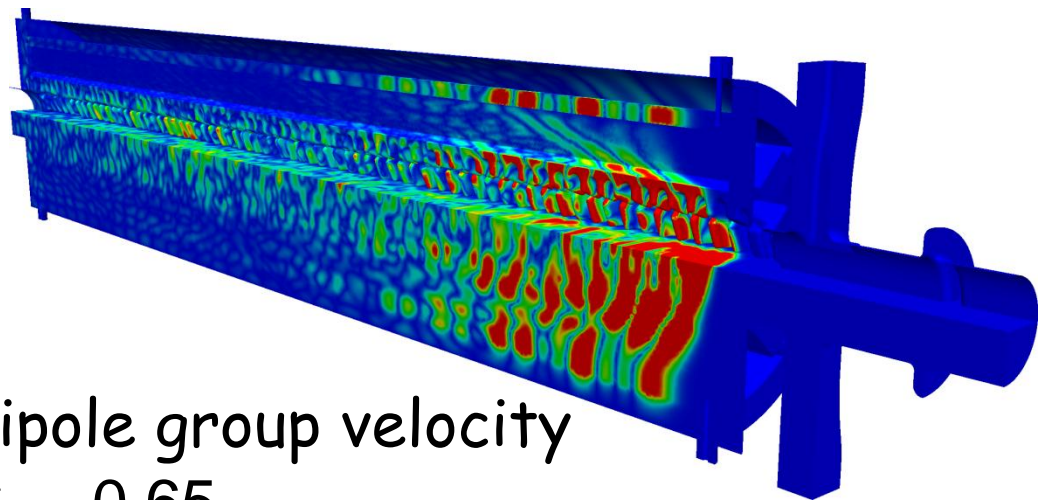
---

T3P is designed to model large structures with highest geometric fidelity via conformal (curved) meshes.

136+2 cells



68+2 cells



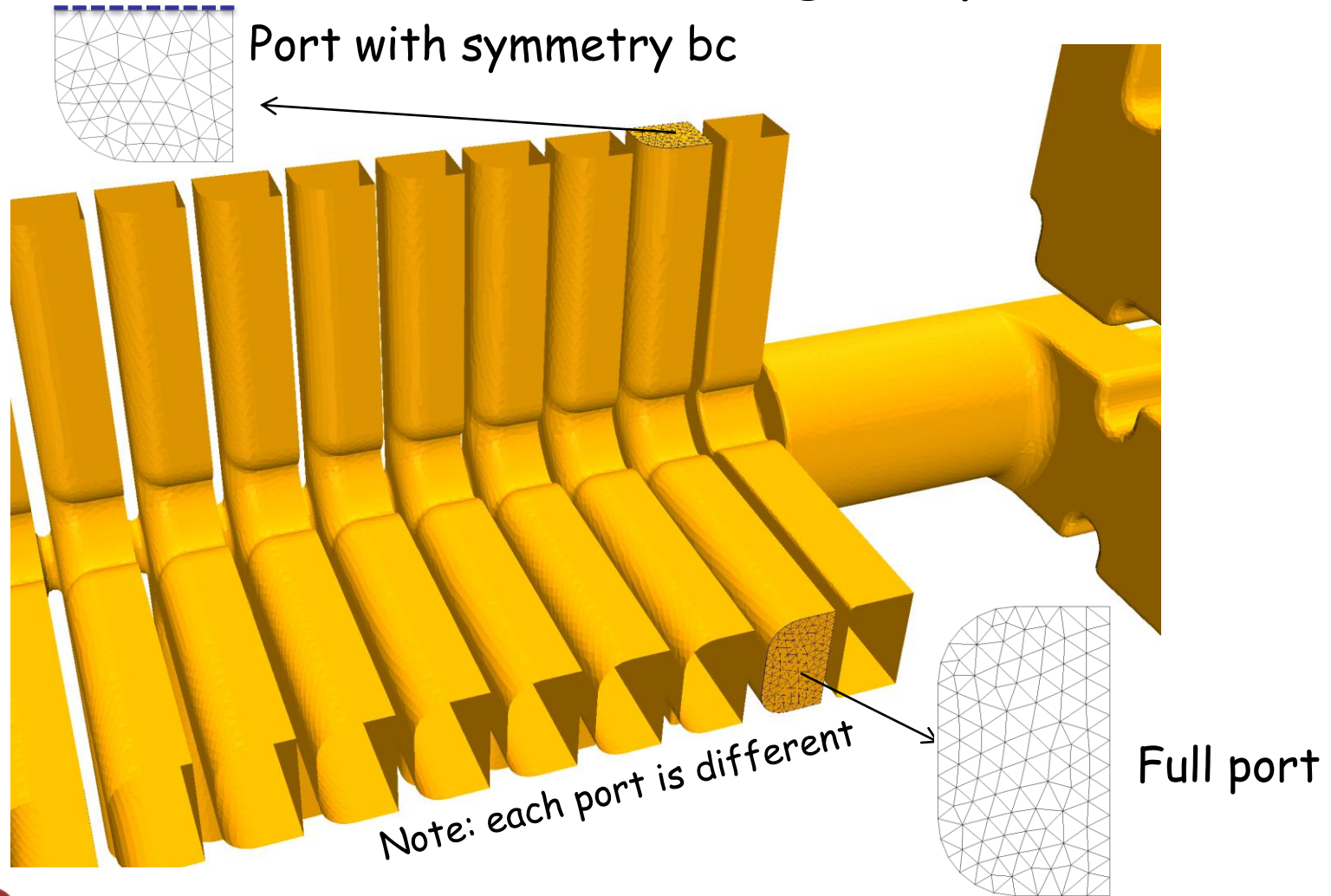
Estimated PETS dipole group velocity  
 $\beta \approx 0.6 \dots 0.65$



# T3P Broadband Waveguide Boundary Conditions

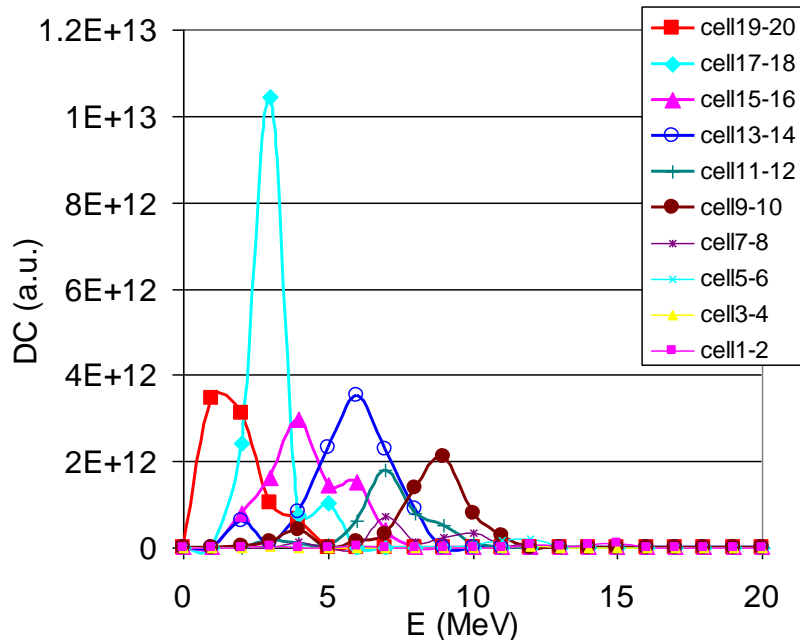
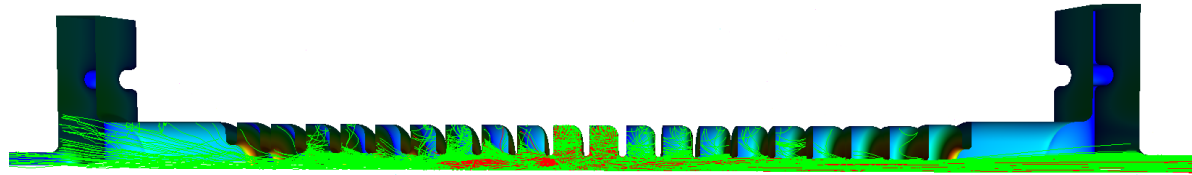
---

## Step 1: Extract 2D mesh of waveguide ports





# Energy of Captured Dark Current vs Location



## Simulation

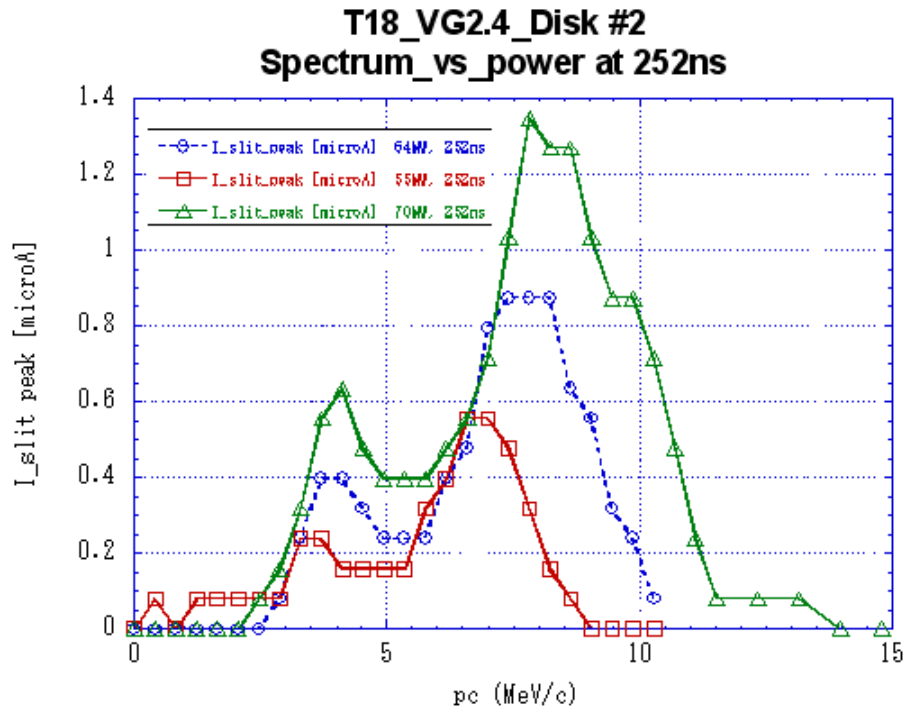
Electron energy as function of emission location.

- $E_{acc}=97\text{MV/m}$ .
- Higher cell number indicates downstream location

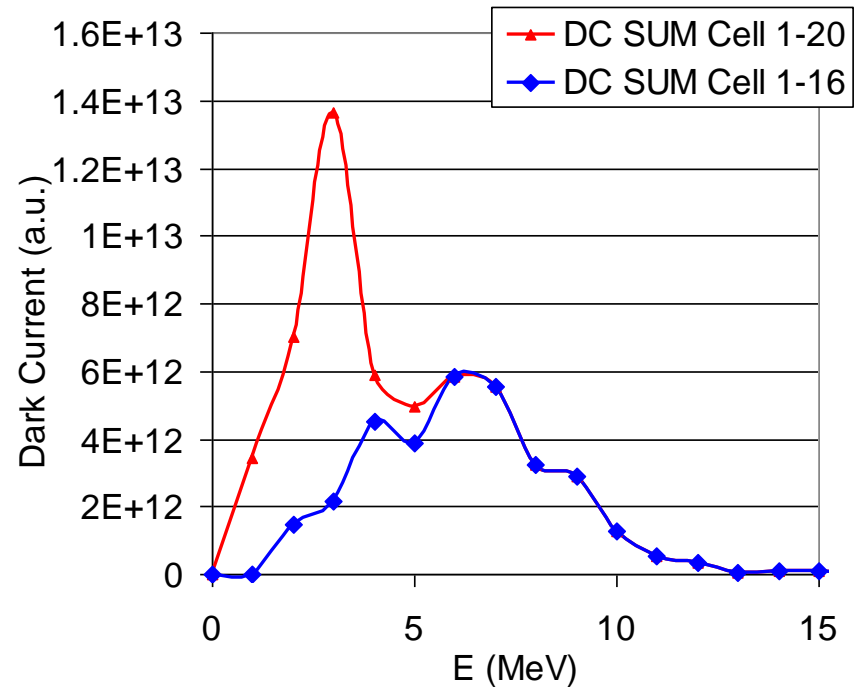
Electrons emitted upstream are accelerated to higher energy (monitored at output end).



# Dark Current Spectrum Comparison



Measured dark current energy spectrum at downstream (need to scale by  $1/(\text{pc})$ )



Spectrum from Track3P simulation, 97MV/m gradient.

“Certain” collimation of beam pipe on dark current is considered in simulation data. More detailed analysis Needed.





# rf absorbers



We need lots and lots of microwave absorbing material- both now and in the long term.

We now *seem* to have a stable supplier of SiC.

But working with SiC seems to be an activity with many surprises.

Our main collaborators in this activity are CIEMAT, EPFL, PSI and Tsinghua University.

We look with interest in developments on HOM dampers for superconducting cavities – for example for energy recovery linacs.





## *S-par Measurements of Material in WG*



### Wave guides

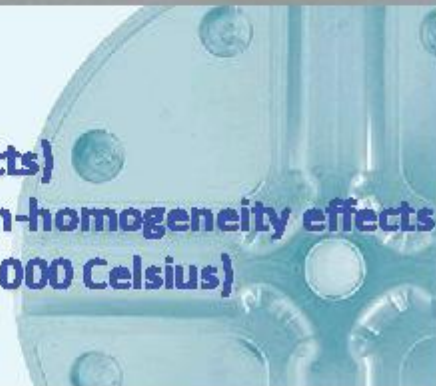
#### **S parameters measurement:**

- HFSS + Measurements  
(Ref. CLIC-NOTE-766)
- Exploring New analysis method



#### **Samples Preparation:**

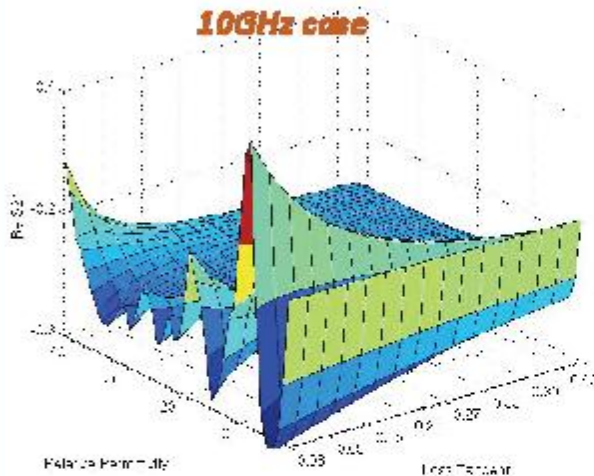
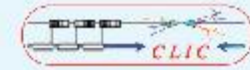
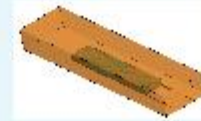
- Machining of samples
  - Different sizes (to define geometry effects)
  - Many samples to have statistics and non-homogeneity effects
- Measurements also after heat treatment (1000 Celsius)



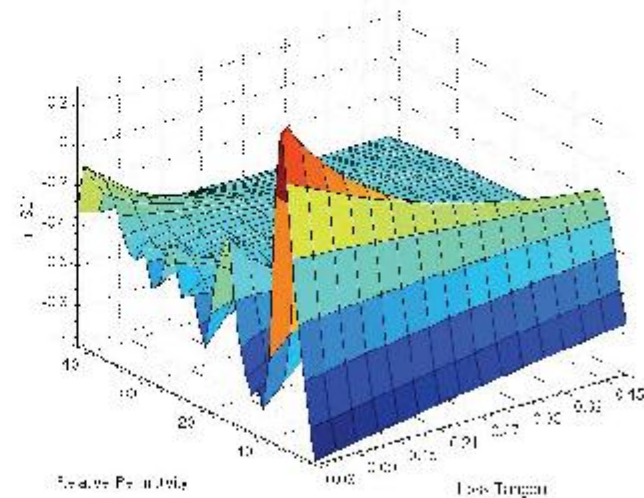




## SURFACE METHOD



**For defined geometry a scan over all possible values of Loss Tangent and Relative Permittivity we have:**  
**Re and Im S21 and Mag S11**

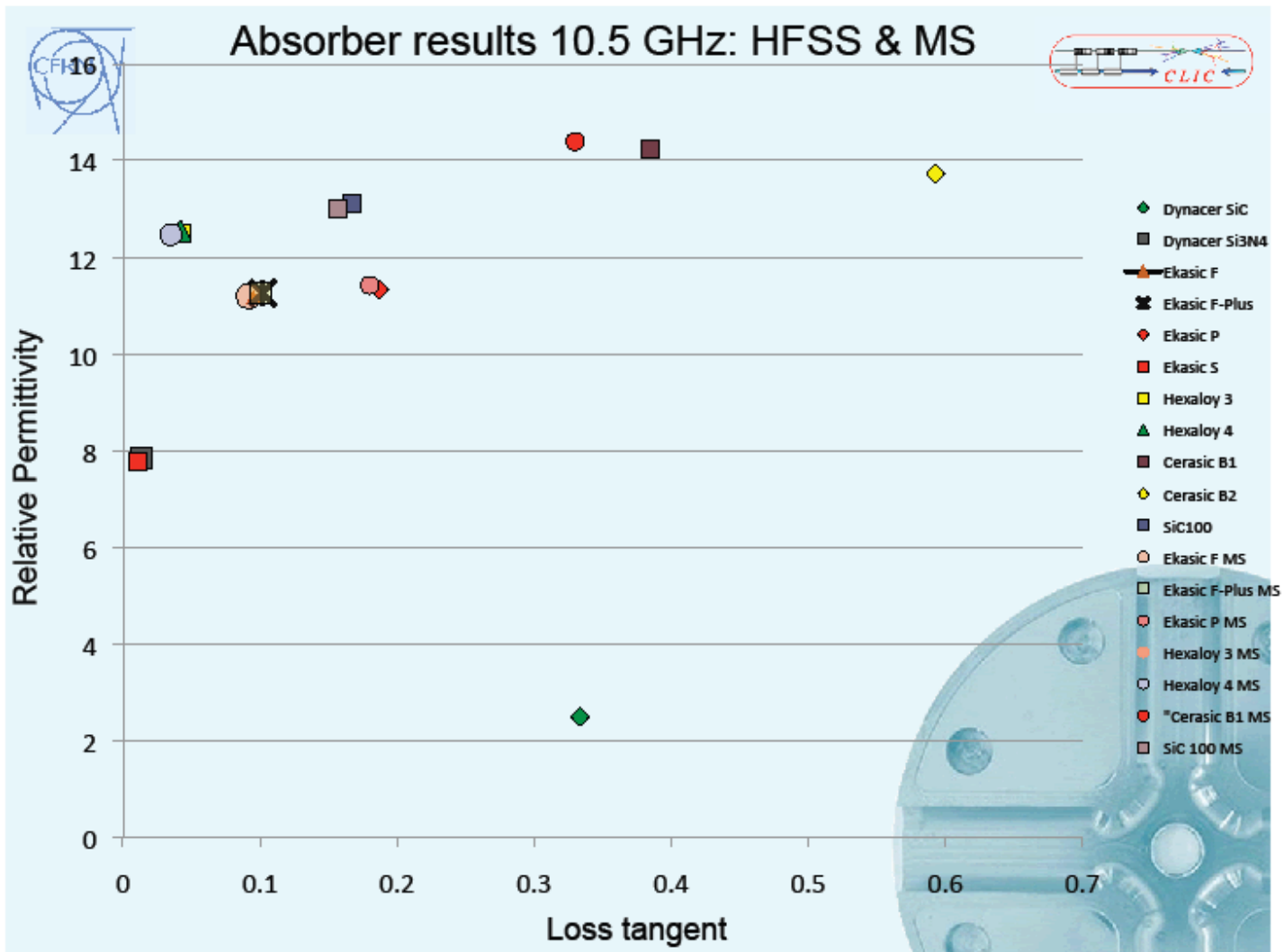


**Measured transmission and reflection coefficients define intercepting plane**

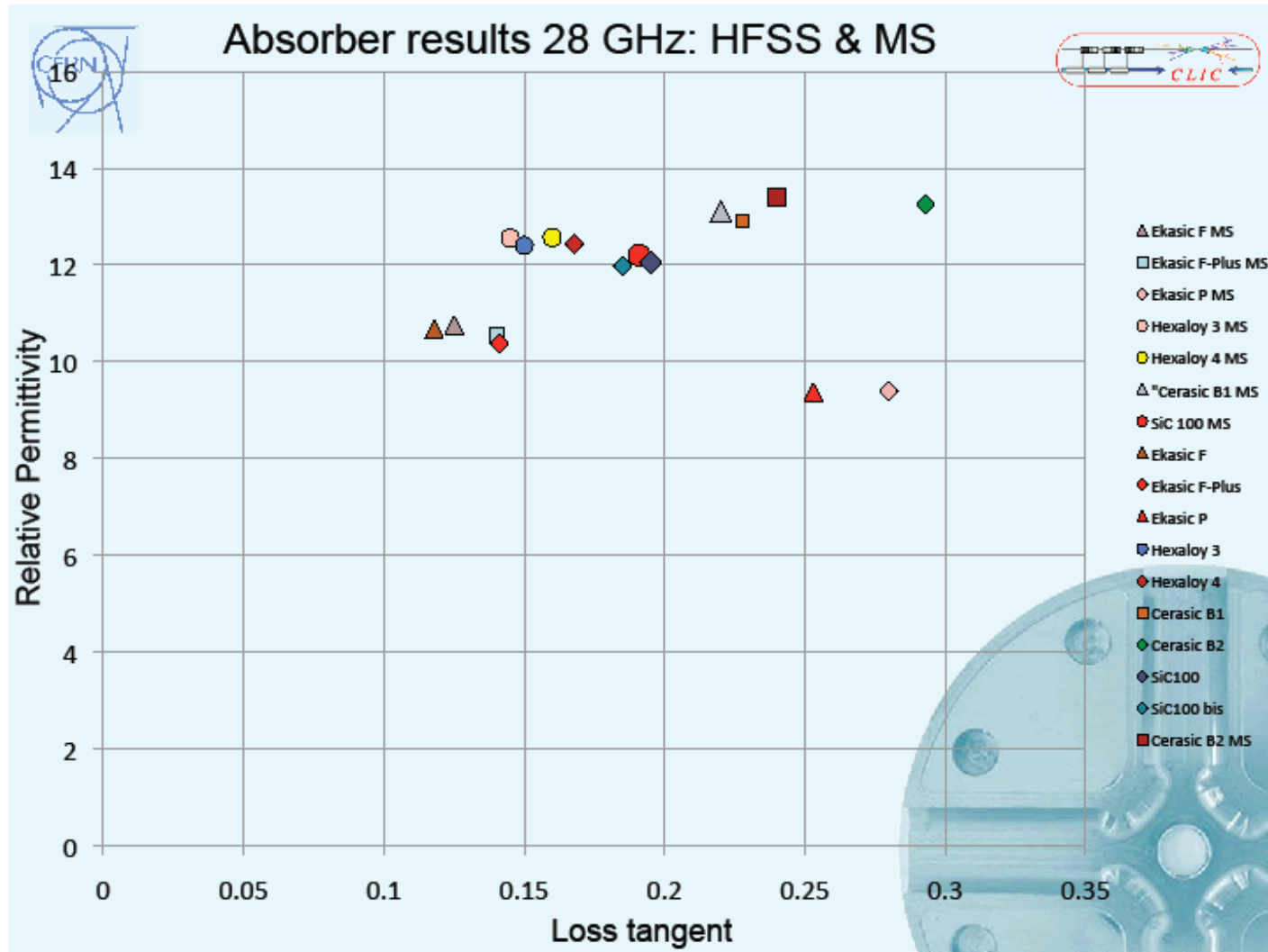
**AT 10GHz  $ReS_{21} = -0.178$  and  $ImS_{21} = 0.064$**   
**Goals come from measurements**















# Simulation of high-power effects



We are promoting a collaboration dedicated to the fundamental study of high-gradient and high-power phenomenon. The main areas are breakdown, pulsed surface heating and high-power rf scaling laws.

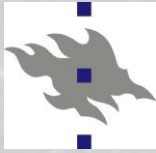
A major breakdown simulation effort is lead by a group at the Helsinki Institute of Physics.

To compliment the simulation effort and rf tests, we have a dc spark system at CERN. Uppsala University is also preparing a dc spark system built into an SEM and ion beam microscope.

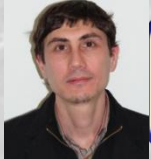
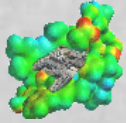
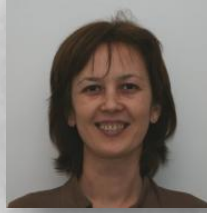
Experimental and simulation efforts are also occurring at the Institute of Applied Physics Sumy, Ukraine.

We are making good progress in understanding how to predict gradients in rf structures in a collaboration between CERN, SLAC and KEK.





# Electrical Breakdown in multiscale modeling approach



**Stage 1:** Charge distribution @ surface  
*Method:* DFT with external electric field

~few fs



**Stage 2:** Atomic motion & evaporation  
+  
Joule heating (electron dynamics)  
*Method:* Hybrid ED&MD model (includes Laplace and heat equation solutions)

~few ns

~ sec/min

**Stage 3a:** Onset of tip growth;  
Dislocation mechanism  
*Method:* MD, Molecular Statics.



**Stage 3b:** Evolution of surface  
morphology due to the given charge  
distribution  
*Method:* Kinetic Monte Carlo

~ sec/hours



**Stage 4:** Plasma evolution, burning of arc  
*Method:* Particle-in-Cell (PIC)

~10s ns

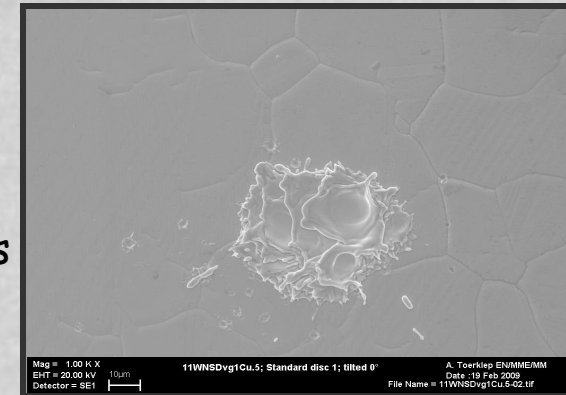


**Stage 5:** Surface damage due to the  
intense ion bombardment from plasma  
*Method:* Arc MD

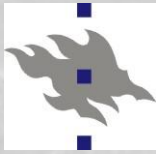
~100s ns



PLASMA  
ONSET







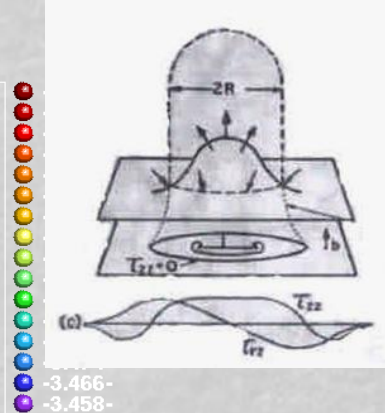
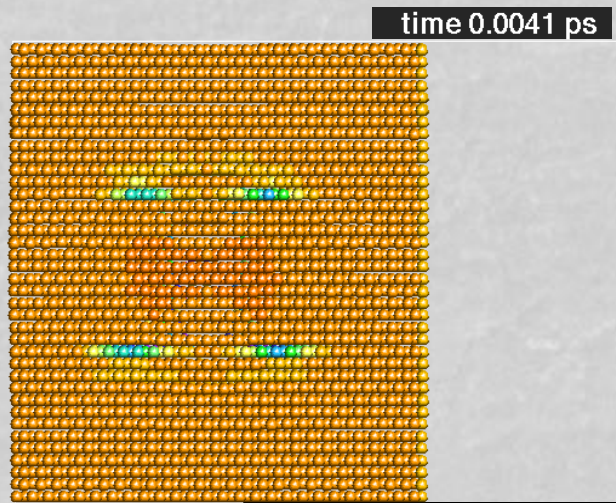
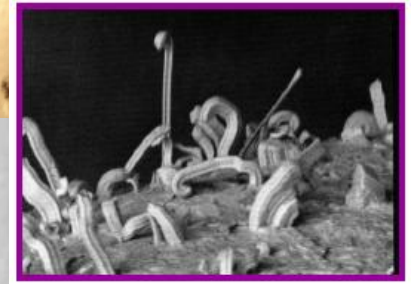
# Step 3a: Are tiny whiskers possible?

**Stage 3a:** Onset of tip growth;  
Dislocation mechanism

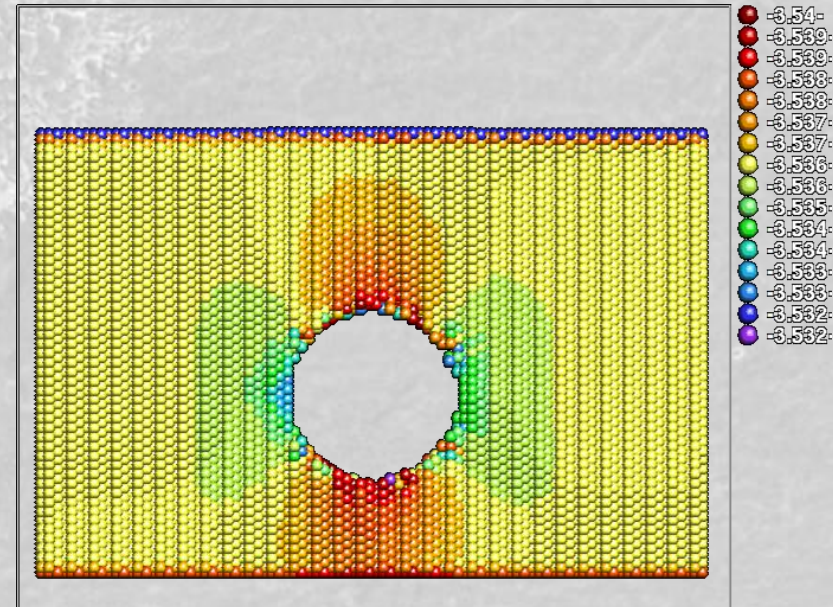
**Method:** MD, Molecular Dynamics



There is a number of mechanisms which might make the dislocations move coherently causing a directed mass transport, thus forming a whisker growth. We are looking for the most probable at our condition.



Aarne Pohjonen and Flyura Djurabekova (2009)

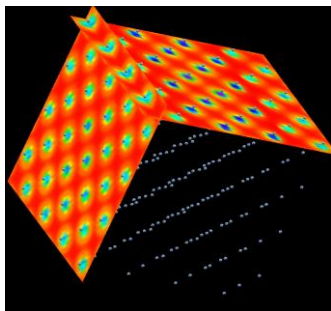
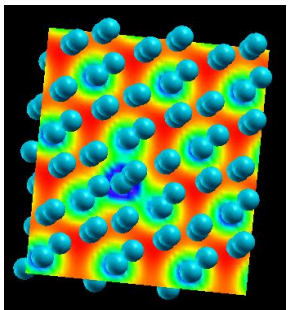
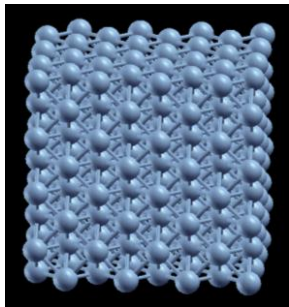


Talk by Aarne Pohjonen in the afternoon



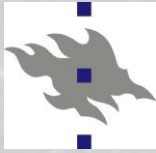


# Stage 1: DFT Method for charge distribution in Cu crystal

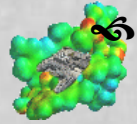


- Writing the total energy as a functional of the electron density we can obtain the ground state energy by minimizing it.
- This information will give us the **properties of Cu surface**
  - Total energy, charge states (as defect energy levels)
- The calculations are done by **SIESTA** (Spanish initiative for electronic structure with thousands of atom)
- The code allows for including an external electric field
- The surface charges under the field are analyzed using the Mulliken and Bader charge analysis





# Stage 2: What about electrons?



At this high electric fields the field emission is non-negligible phenomenon.



Electrons escaping from the surface with the significant current will heat the sharp features on the surface, causing eventually their melting.

The change of the temperature (kinetic energy) due to the Joule heating and heat conduction calculated by 1D heat equation

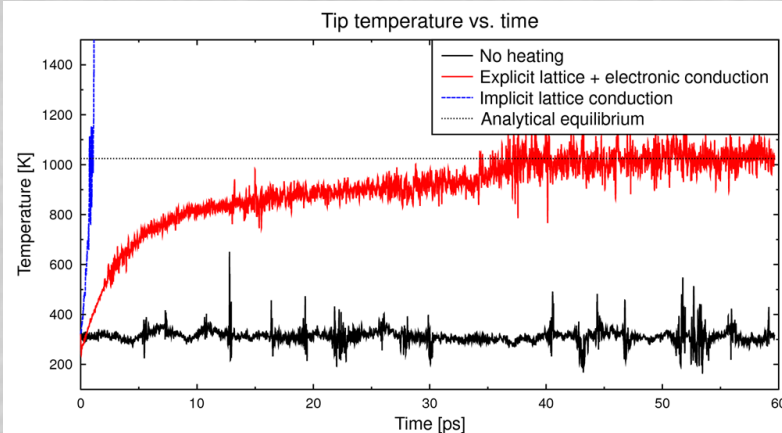
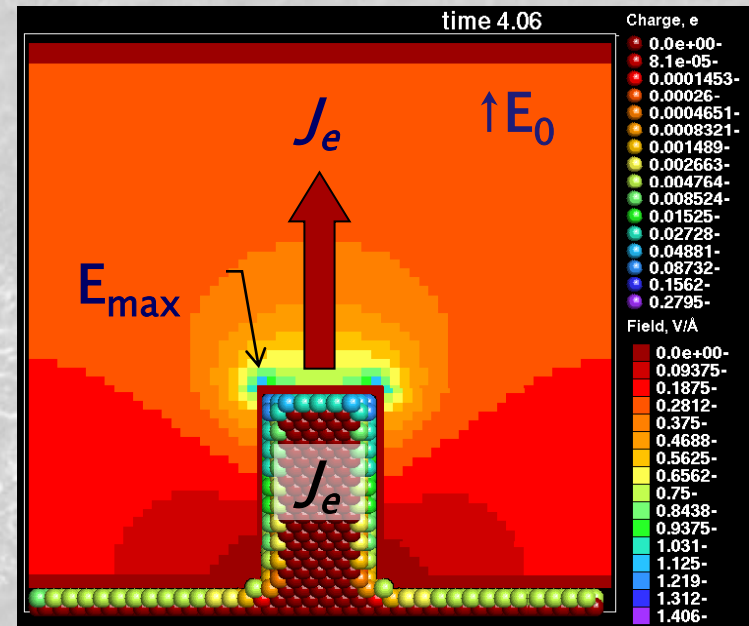
$$\frac{\partial T(x,t)}{\partial t} = \frac{K}{C_v} \frac{\partial^2 T(x,t)}{\partial x^2} + \frac{\rho(T(x,t))J^2}{C_v}$$

More details at Poster by Stefan Parviainen

Flyura Djurabekova, HIP, University of Helsinki

Stage 2: Atomic motion & evaporation  
+  
Joule heating (electron dynamics)

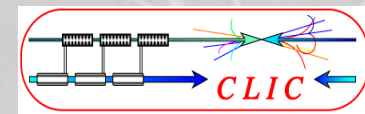
**Method:** Hybrid ED&MD model (includes Laplace and heat equation solutions)







# Overview of the CLIC R&D program on breakdown continued

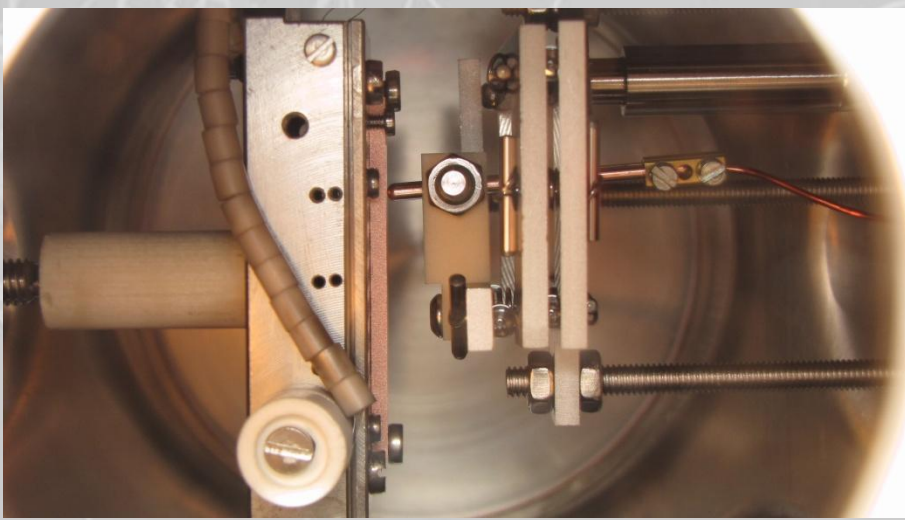


In order to increase our experimental capacity (and constrain speculation) we have also invested in two **dc** spark systems.

Advantages: The systems and samples are far cheaper than for rf. Easier to introduce alternative materials, new diagnostics, test ideas like temperature dependence etc. Easier to geometry to think about and to simulate.

But aren't rf and dc sparks "different?" Mostly not and where they are - the total voltage, single polarity – the differences are telling us a lot.

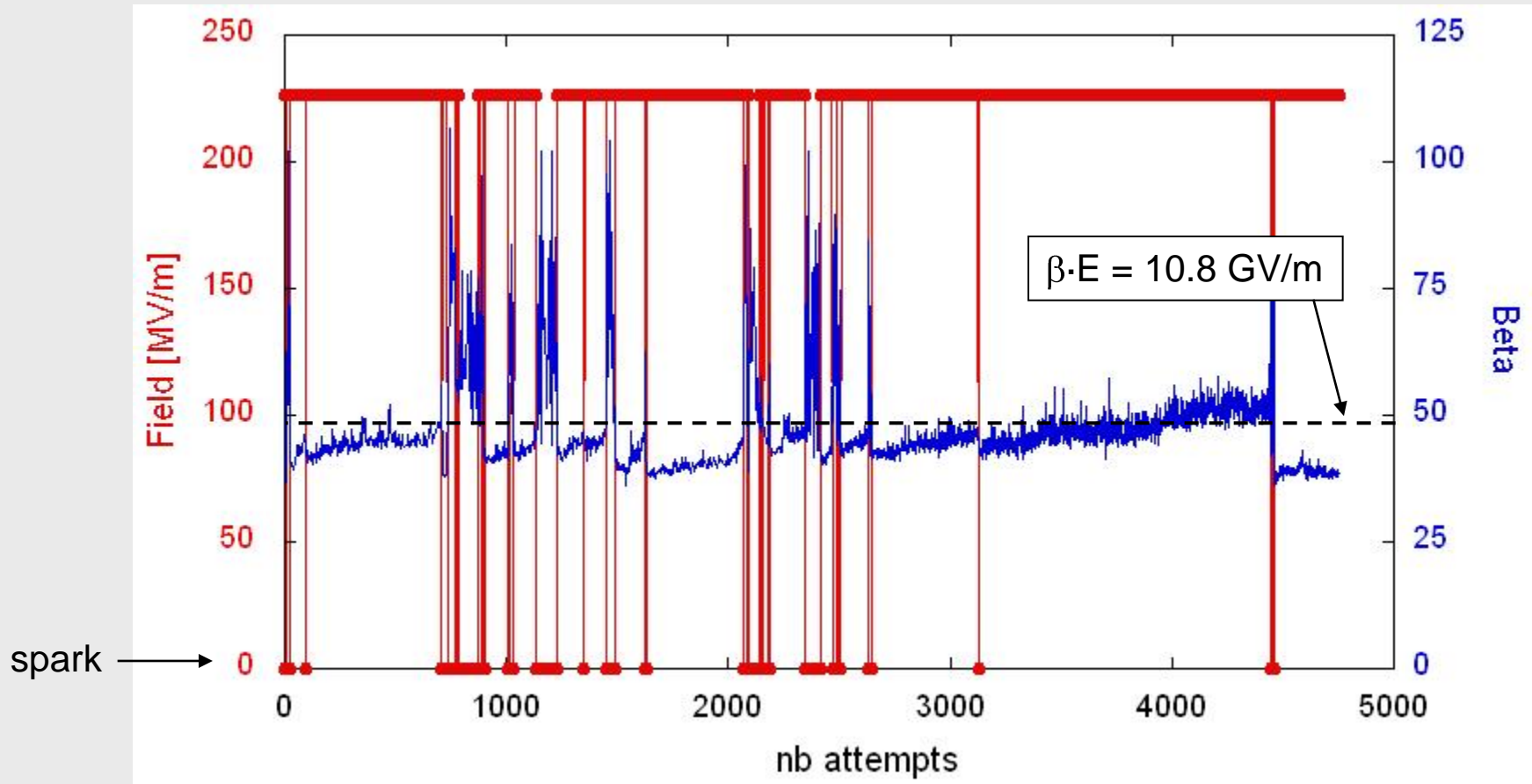
Haven't lots of people done dc tests before? Yes, but we have many specific questions especially, what is the breakdown rate vs. field dependence and where does it come from? Also practical stuff like: What is our copper like or what effect does this surface treatment have?



Sergio Calatroni, 14:00 today



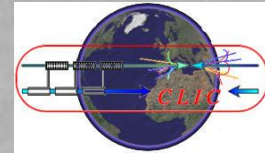
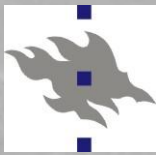
# Evolution of $\beta$ during BDR measurements (Cu)



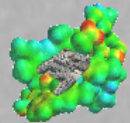
- breakdown as soon as  $\beta > 48$  ( $\leftrightarrow \beta \cdot 225 \text{ MV/m} > 10.8 \text{ GV/m}$ )
- consecutive breakdowns as long as  $\beta > \beta_{\text{threshold}}$

→ length and occurrence of breakdown clusters  $\leftrightarrow$  evolution of  $\beta$

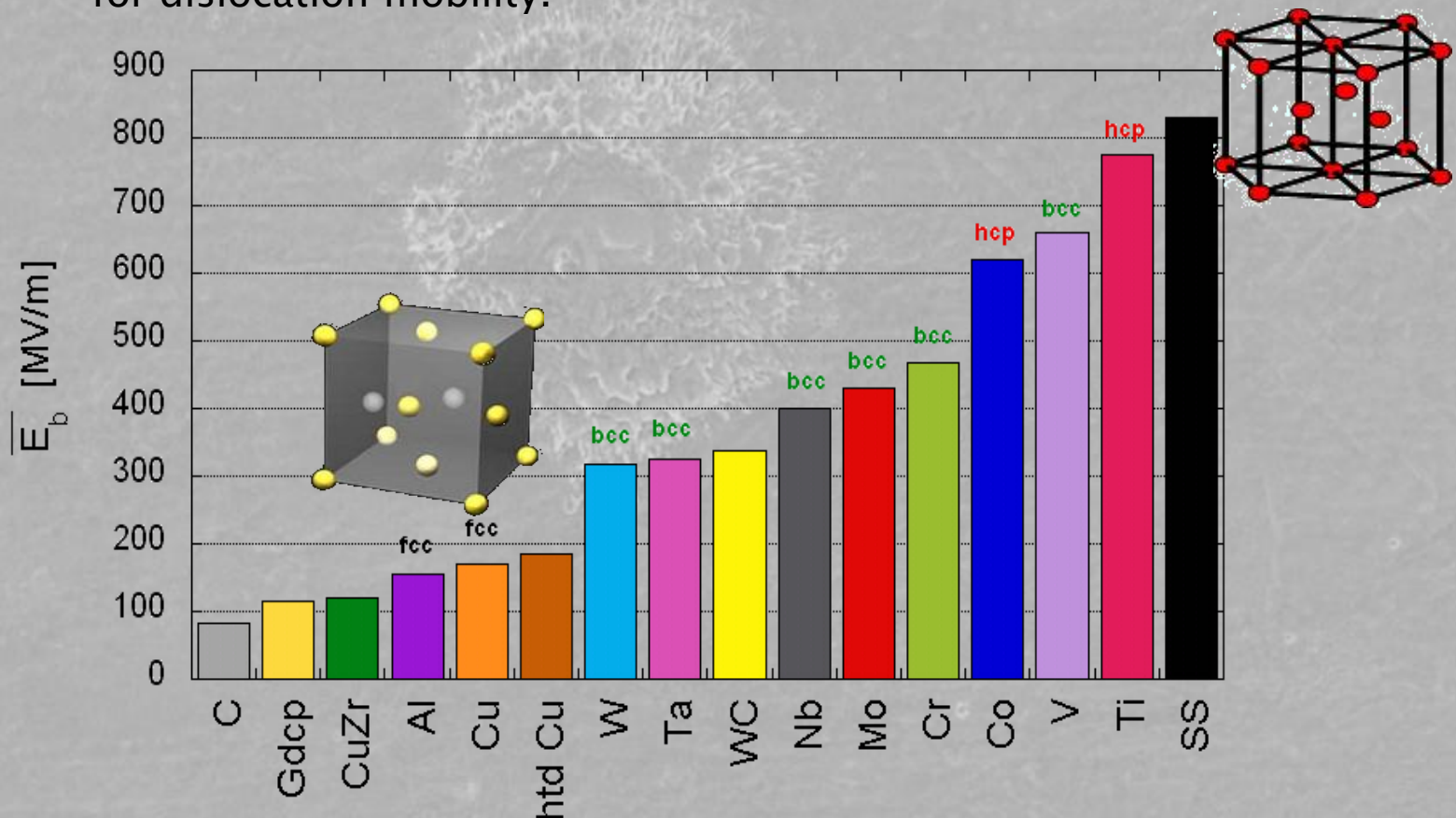




## Recent experiment at CERN: CLIC-note



- ✎ The dislocation motion is strongly bound to the atomic structure of metals. In FCC (face-centered cubic) the dislocation are the most mobile and HCP (hexagonal close-packed) are the hardest for dislocation mobility.





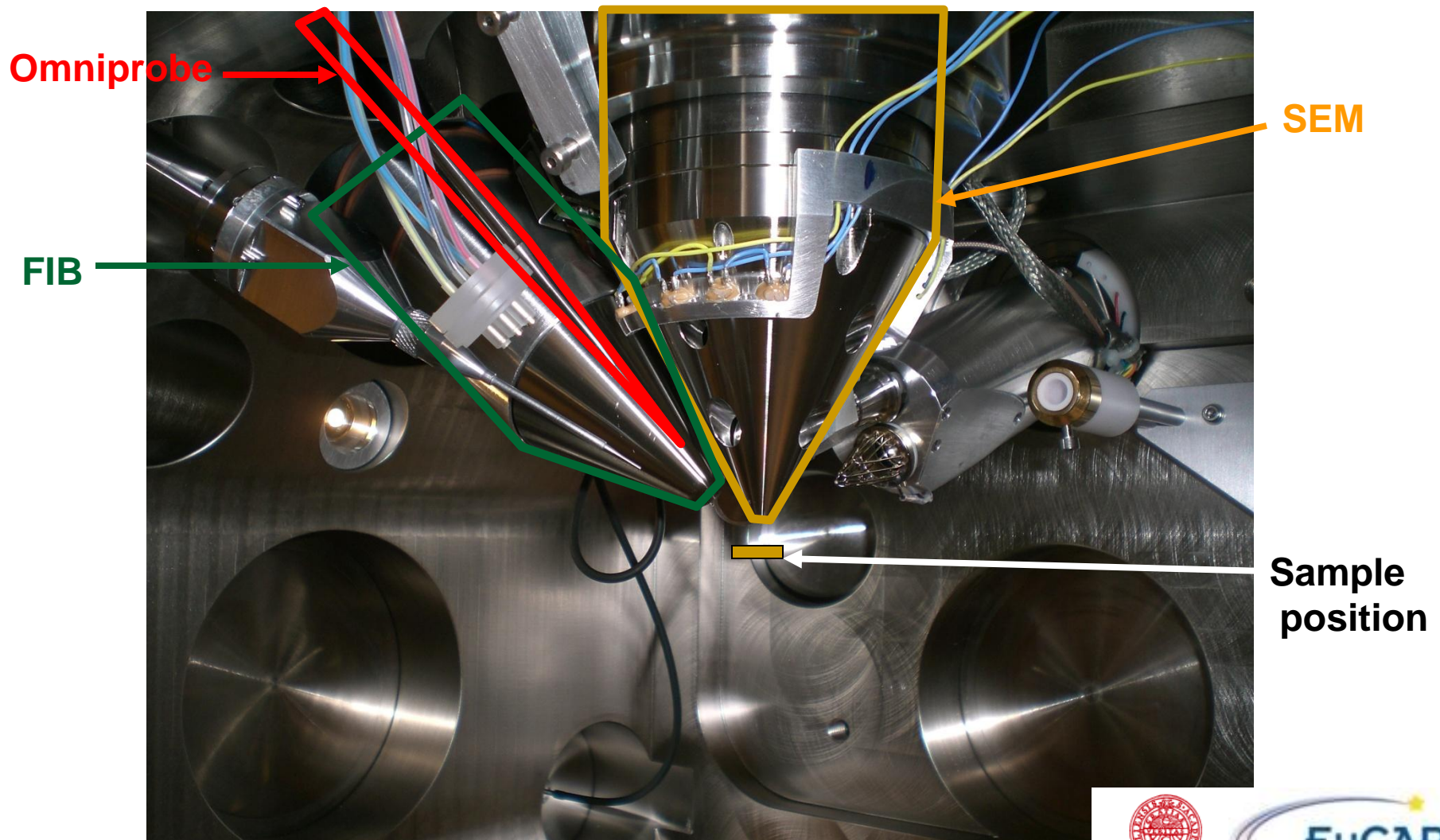
# Instruments: FIB



- FIB: combined Focussed Ion Beam and SEM
- -> **Create** surface corrugations, pillars and tips with Focussed Ions, **Observe** surface both by SEM and by FIB
- 3D structure fabrication by FIB milling
- EDX (big cylinder)
- Omniprobe manipulator as a HV tip



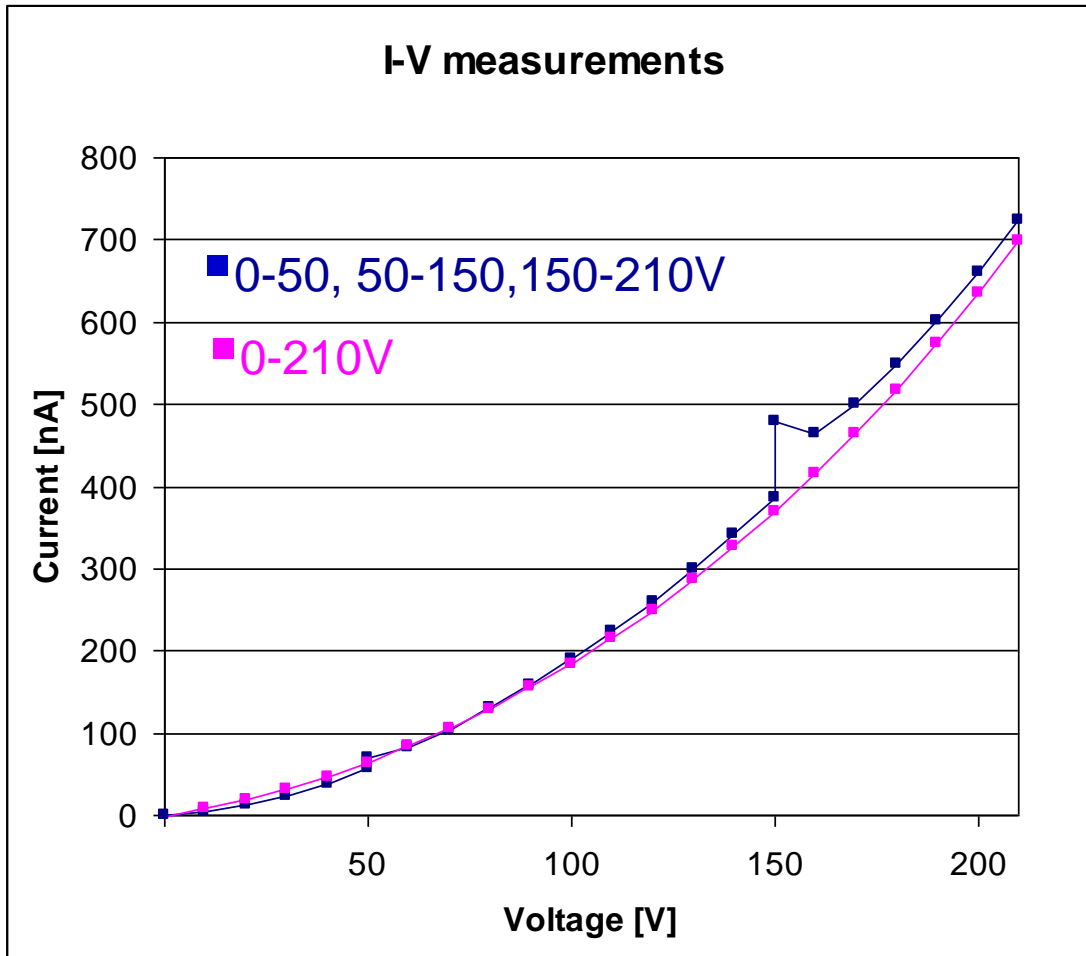
# Instruments: inside view of FIB



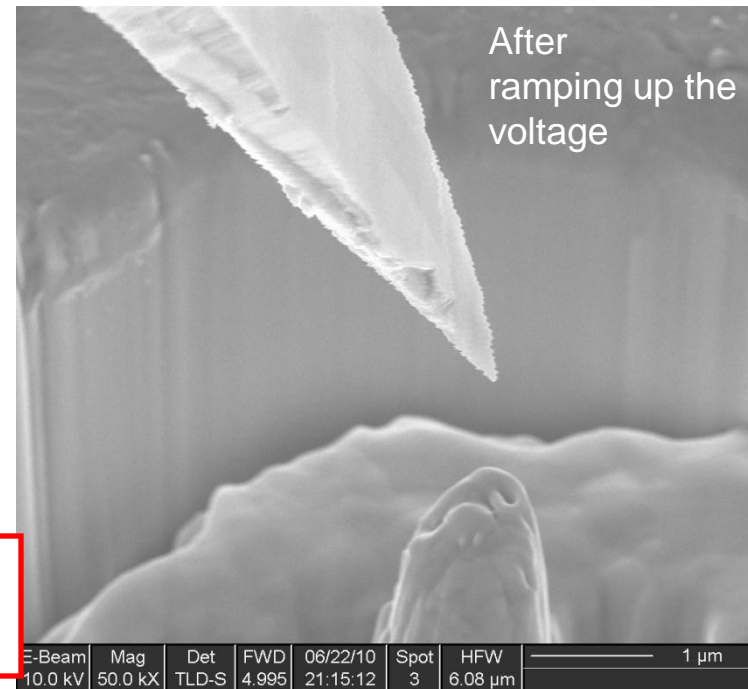
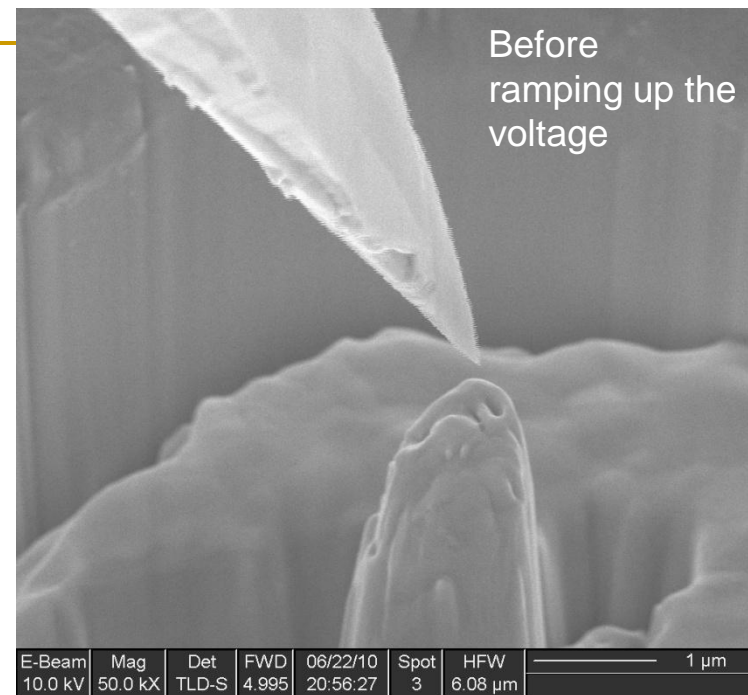


# I-V measurements

June 22, distance ~ 250-800nm

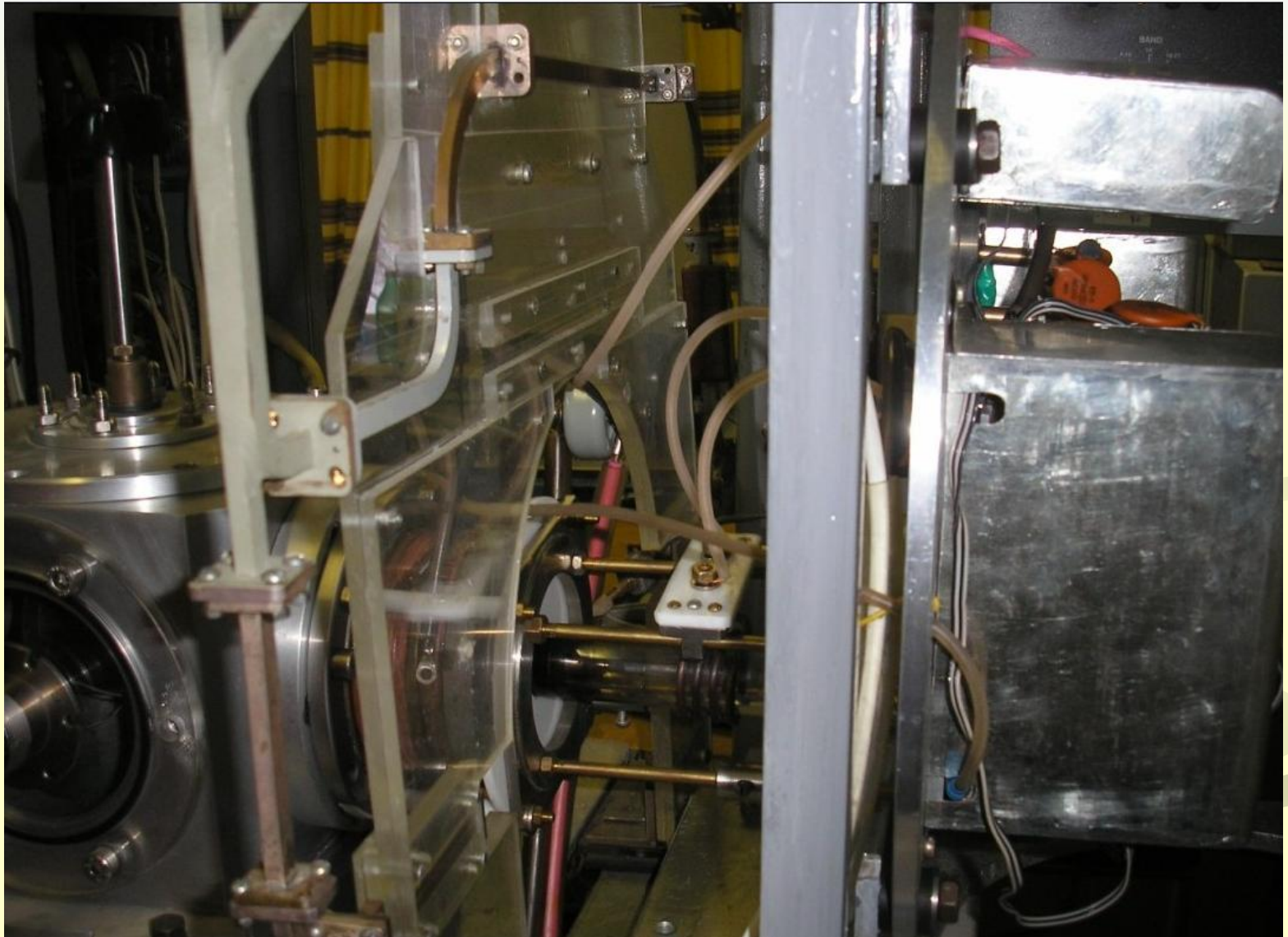


-Distance between the needle and the pillar changes  
-“Relaxation” of current has been observed





## Setup for measurement of plasma parameters





# Fluid model

## Equations system of the two fluids hydrodynamics

$$\begin{aligned}
 \operatorname{div}(n_i \mathbf{u}_i) &= n_i (\langle v^i \rangle - \langle v^r \rangle) \\
 \operatorname{div}(n_i \mathbf{u}_i \mathbf{u}_i) &= \frac{Z_i e n_i}{m_i} \left( -\nabla \varphi + \frac{1}{c} [\mathbf{u}_i \times \mathbf{B}_0] \right) - \frac{1}{m_i} \nabla(n_i T_i) - n_i \frac{\delta \mathbf{u}_i}{\delta t} \\
 \operatorname{div}(n_e \mathbf{u}_e) &= \operatorname{div}(n_i \mathbf{u}_i) \\
 \operatorname{div}(n_e \mathbf{u}_e \mathbf{u}_e) &= -\frac{e n_e}{m_e} \left( -\nabla \varphi + \frac{1}{c} [\mathbf{u}_e \times \mathbf{B}_0] \right) - \frac{1}{m_e} \nabla n_e T_e - n_e \frac{\delta \mathbf{u}_e}{\delta t} \\
 \operatorname{div} \left( \mathbf{q}_e + \frac{5}{2} n_e \mathbf{u}_e T_e + n_e \mathbf{u}_e \frac{m_e u_e^2}{2} \right) &= -e n_e \mathbf{u}_e \nabla \varphi + P_{abs} + \left( \frac{\delta(n \langle K \rangle)}{\delta t} \right)_{ei} + \left( \frac{\delta(n \langle K \rangle)}{\delta t} \right)_{ea}
 \end{aligned}$$

## Poisson equations

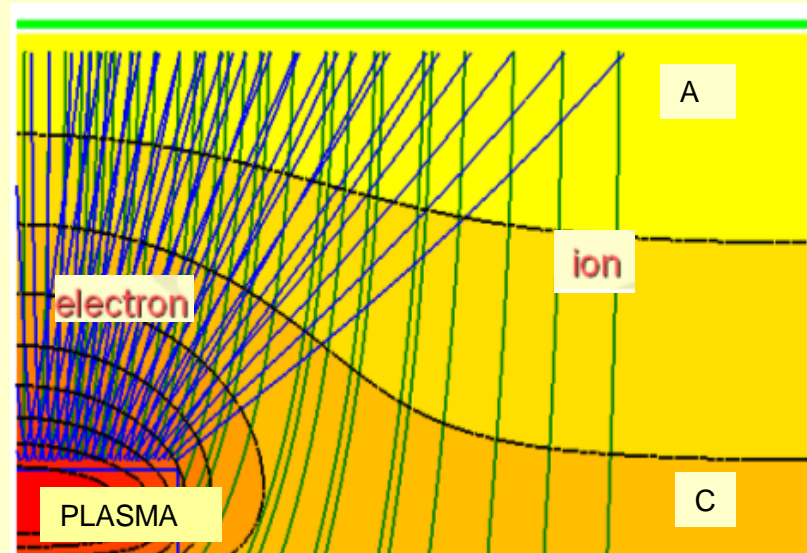
$$-\nabla(\nabla \varphi) = \rho / \epsilon_0;$$

$$\rho = e(n_+ - n_- - n_e).$$

## Equation of motion

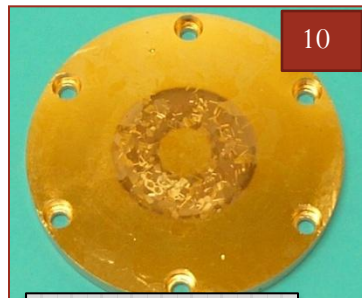
$$n_i \frac{\delta \mathbf{u}_i}{\delta t} = \frac{1}{m_i} (\mathbf{R}_{ia} + \mathbf{R}_{ie} + \mathbf{R}_{ie}^T),$$

$$\mathbf{R}_{ia} = -\mu_{ia} \nu_{ia} \mathbf{u}_i,$$



Mordyk, S.; Alexenko, O.; Miroshnichenko, V.; Storizhko, V.; Stepanov, K.; Olshansky, V. Investigation of rf power absorption in the plasma of helicon ion source//Review of Scientific Instruments, Volume 79, Issue 2, pp. 02B907-4 (2008).





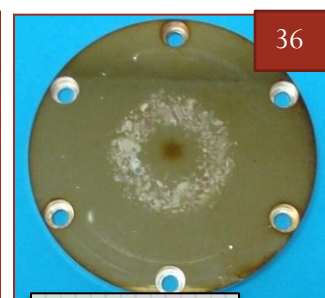
Cu101 (SLAC)



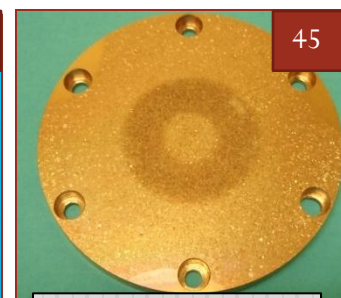
KEK3 (KEK)



HIP2 (KEK)



HIP1 (KEK)



CuZr2-2 (CERN)



CuCr101 (SLAC)



Single Crys Cu (KEK)



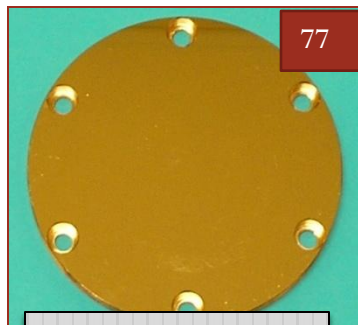
E-Dep. Cu (KEK)



AgPCu (KEK)



Glidcop4-2 (CERN)



CuZr3-2 (CERN)



CuAg5 (SLAC)



CuAg1 (KEK)

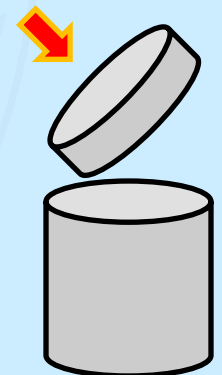
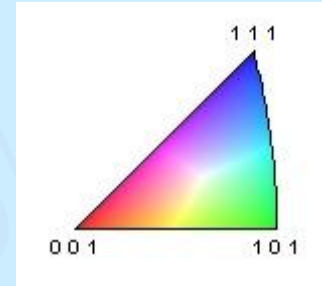
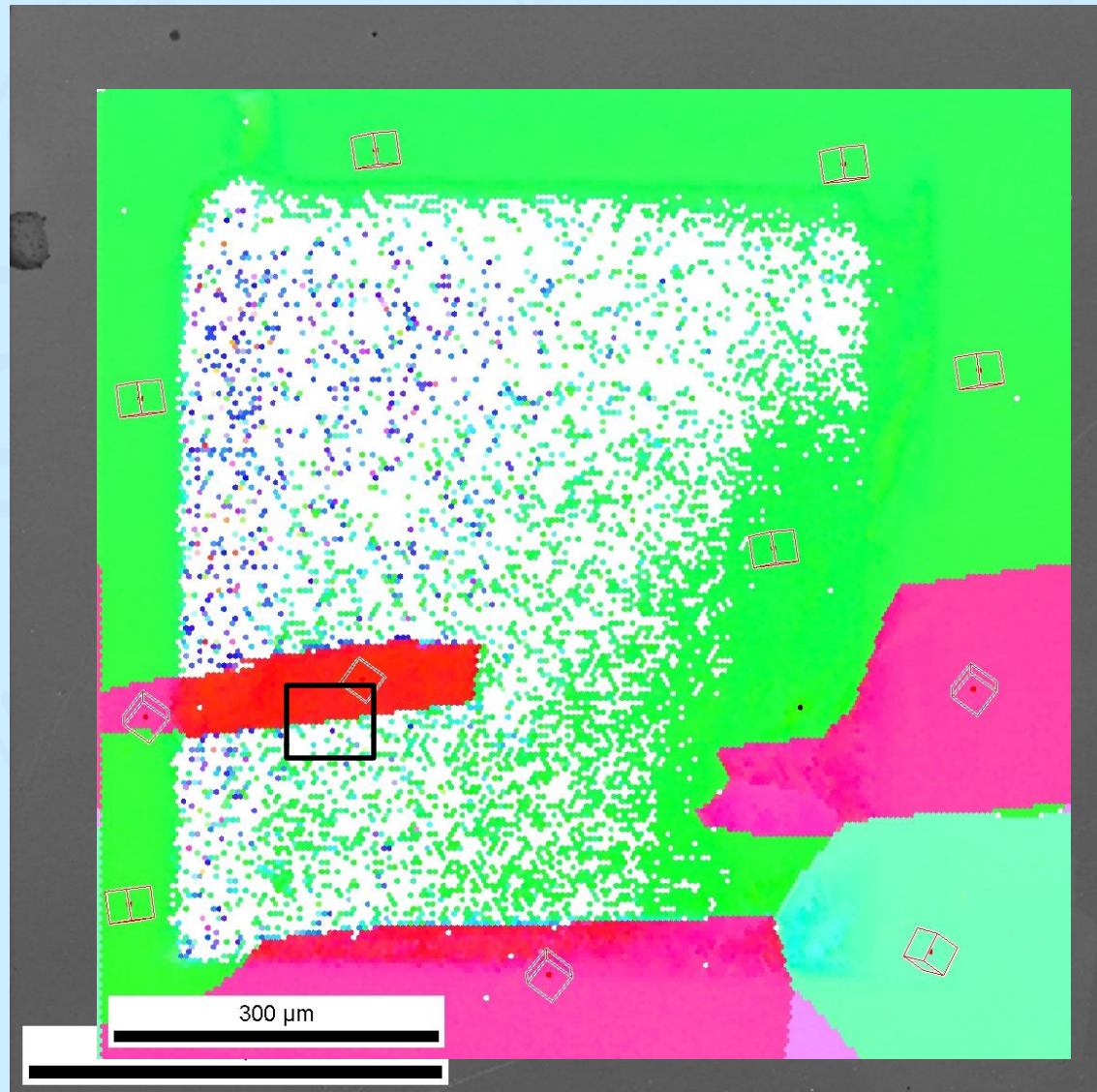
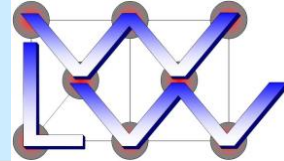


CuCr102 (SLAC)



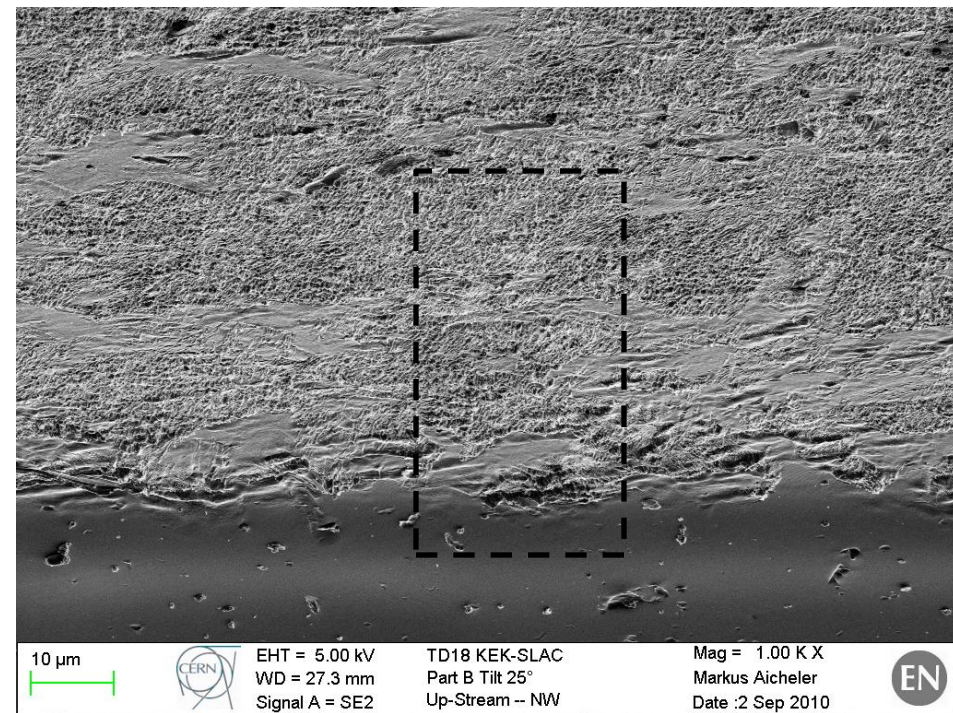
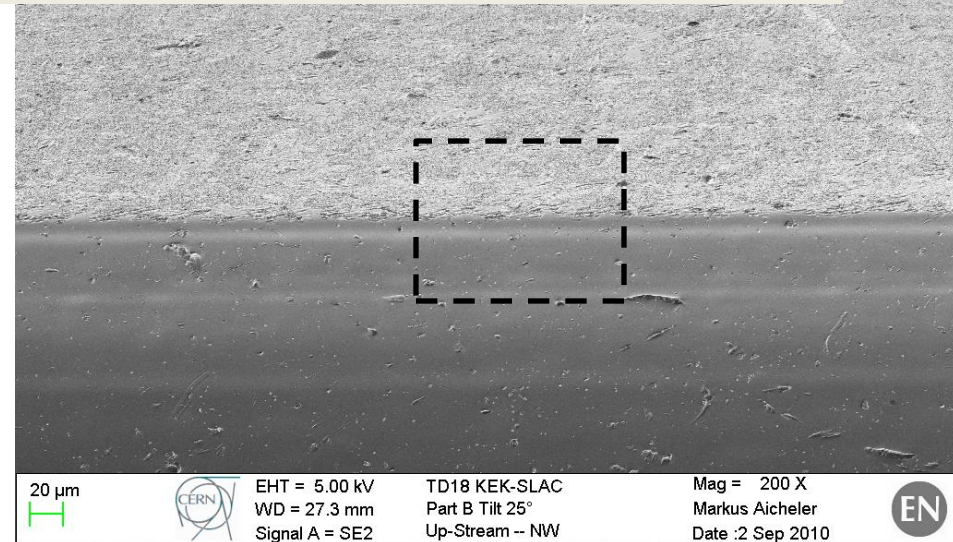
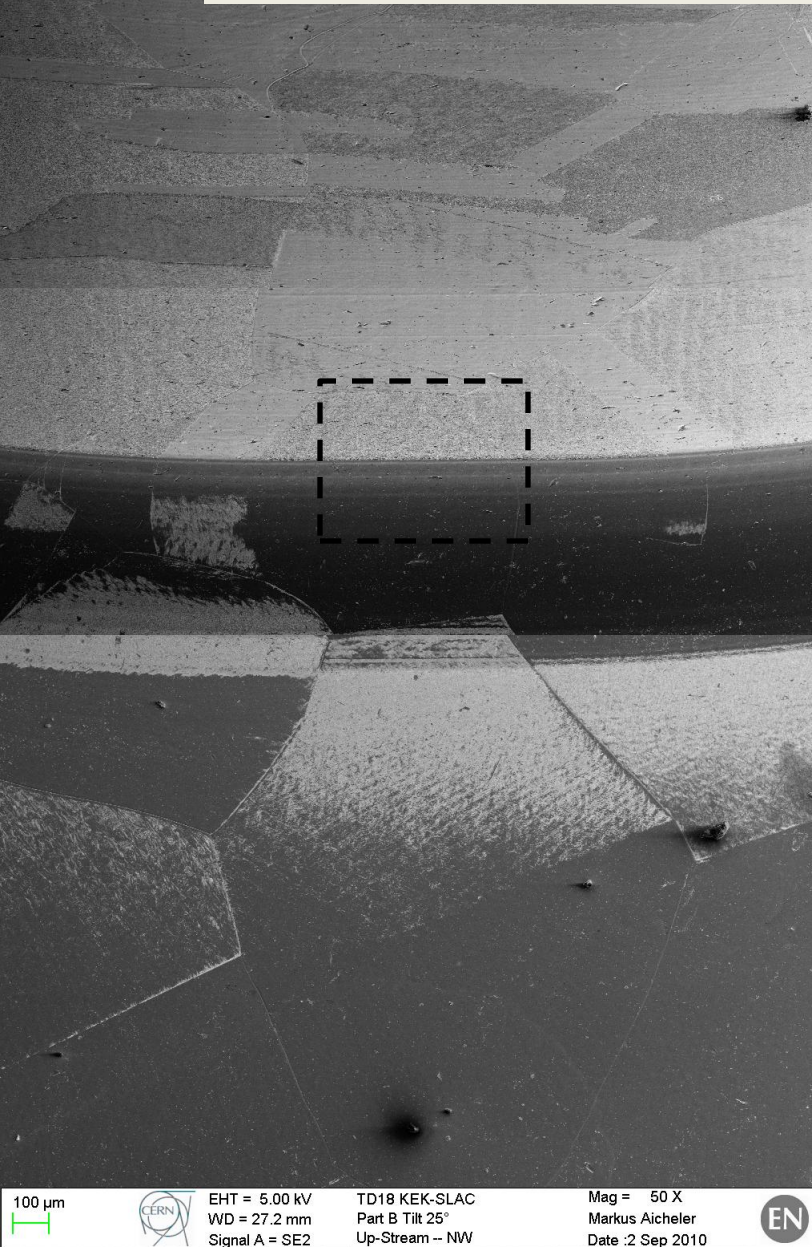
Glidcop4-1 (CERN)







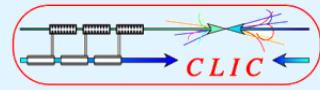
# TD18 – pulsed surface heating in a travelling wave structure







# High-power rf theory and simulation effort

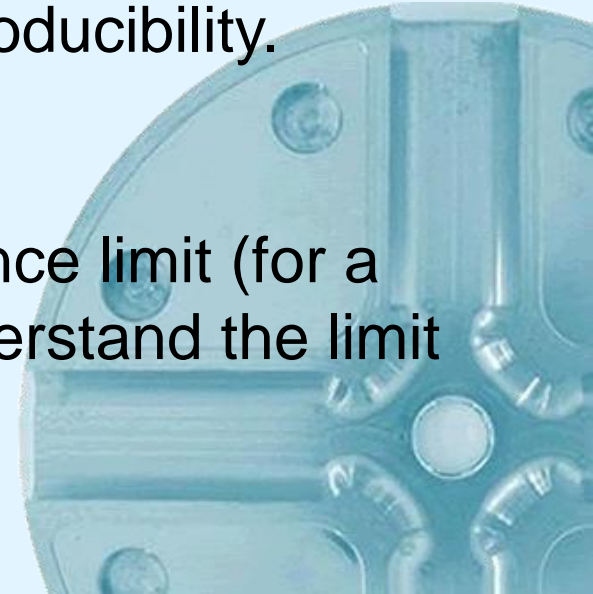


Over the past couple of decades computational tools have developed to the point that we can now accurately design complex, 3-D and even multi-moded rf structures.

The ability to predict high-power performance has lagged behind:

- A lot depends on preparation. But NLC/JLC made enormous progress in improving performance and reproducibility.
- The phenomena are extremely complex.

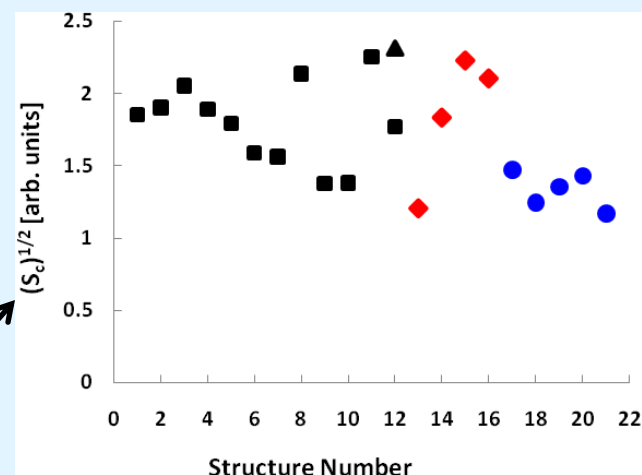
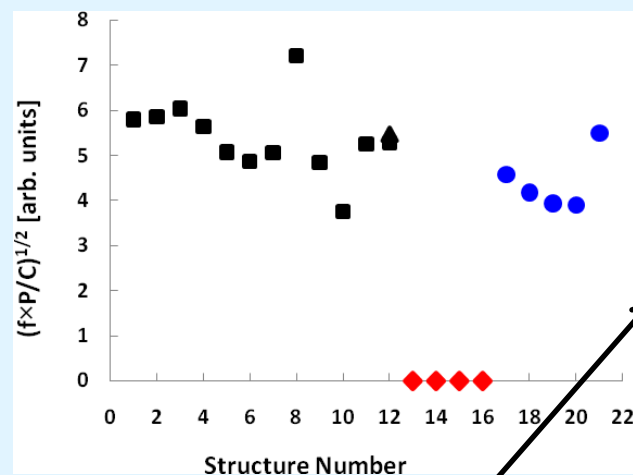
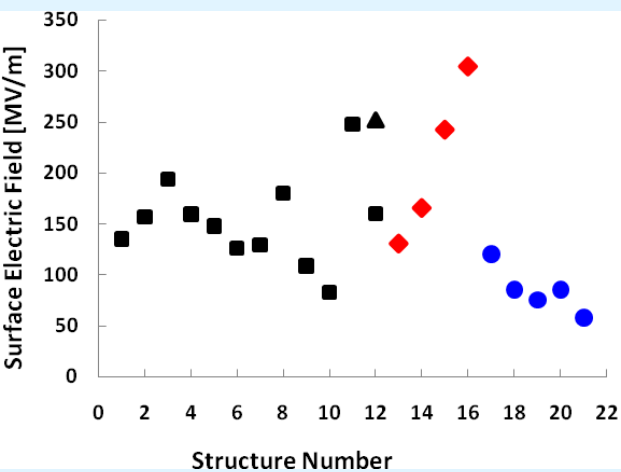
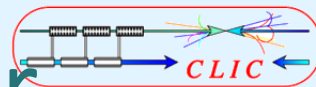
CLIC aims to run very close to the performance limit (for a given breakdown rate) so we had better understand the limit pretty well.







# $S_c$ : high-power design parameter



X-band and 30 GHz,  
pulses of the order of  
100 ns.  
Travelling and standing  
wave

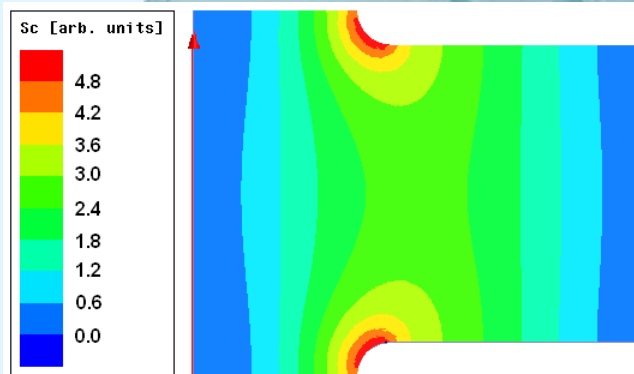
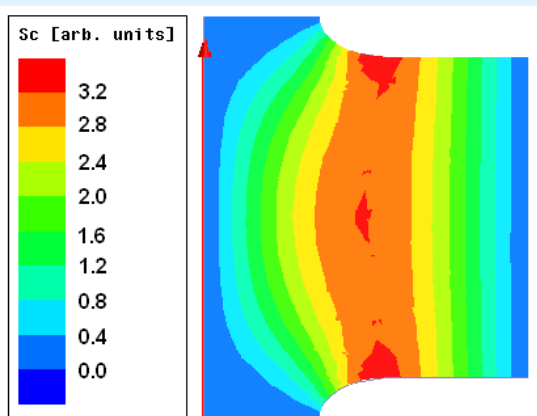
Related to the complex Poynting vector:

$$S_c = \Re \left\{ \vec{S} \right\} \pm g_c \cdot \Im \left\{ \vec{S} \right\}$$

Travelling wave

Standing wave

W. Wuensch



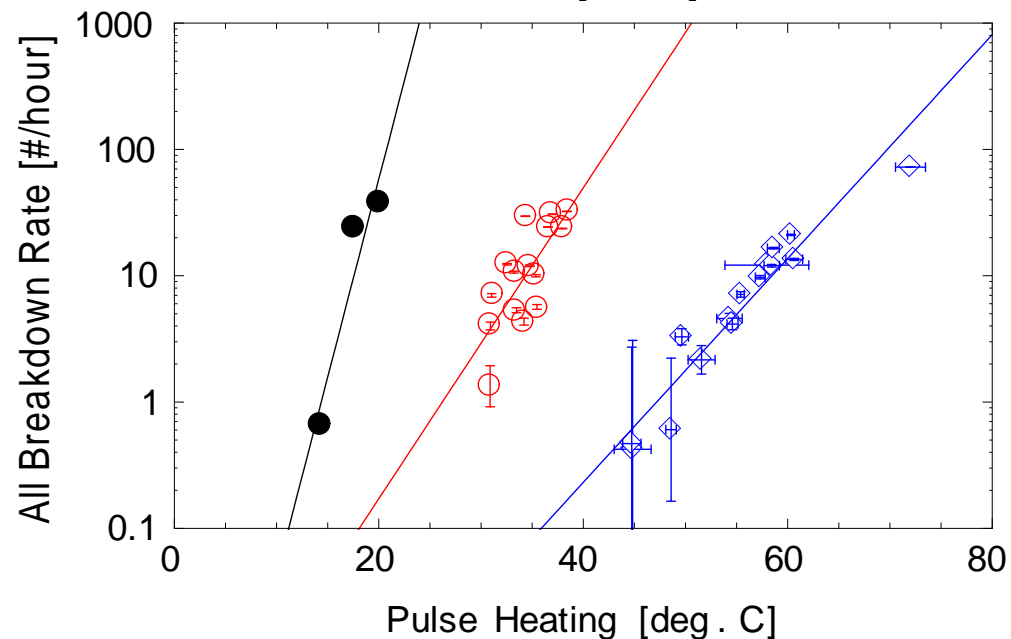
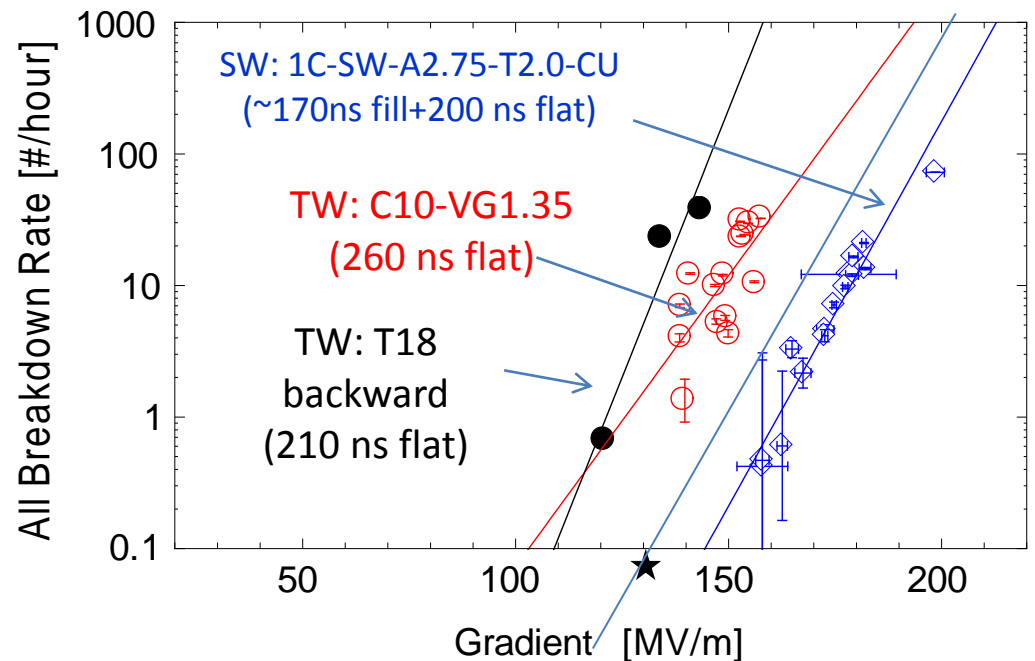


# Geometrical studies

**TW vs. SW:** At low breakdown rate  $< 5 \cdot 10^{-5}$ /per pulse/meter ( $< 10$  per hour@60Hz) the statistical behavior of the SW and low group velocity TW structures is very similar but TW structures has  $\sim 20$ -30% lower gradient and about 2 times lower peak pulse heating.

**Valery Dolgashev**

Breakdown rate vs. gradient and pulse heating for one SW and two TW structures with  $\sim 3$ mm aperture



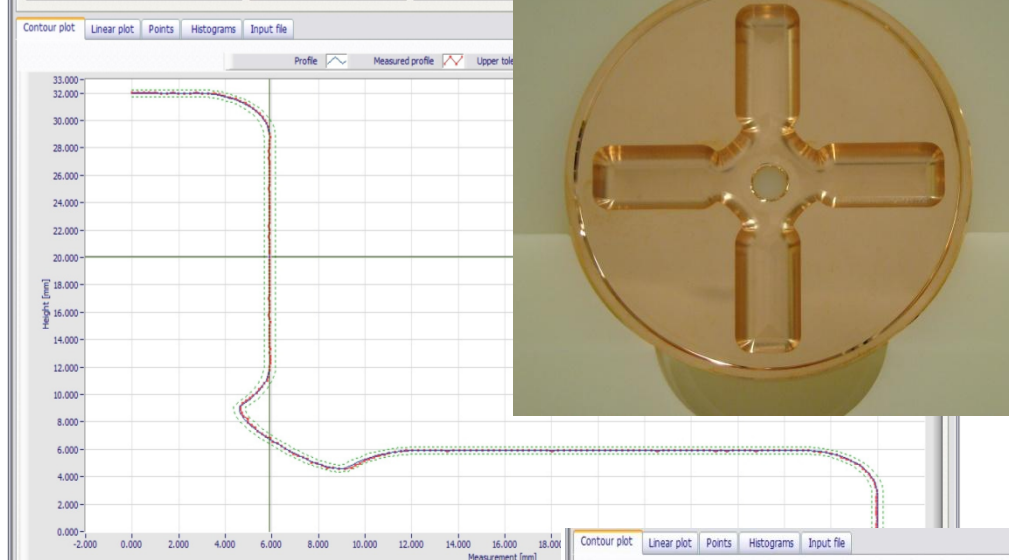
C10 and T18 TW structures: R. Zennaro *et al.*, *Design and Fabrication of CLIC test structures*, LINAC08



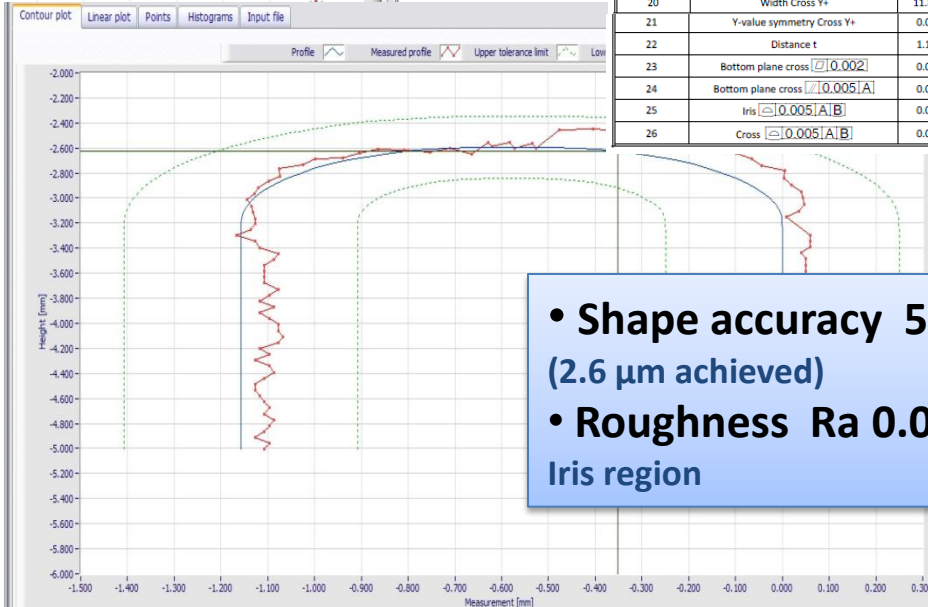
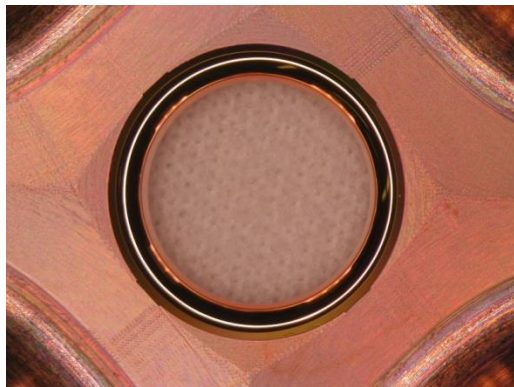


# DETUNED DAMPED DISK FROM VDL (TD24)


germana.riddone@cern.ch



Zeiss CMM, free state measurement



- Shape accuracy 5  $\mu\text{m}$  (2.6  $\mu\text{m}$  achieved)
  - Roughness Ra 0.025
- Iris region



Enabling Technologies Group

Inspection Report

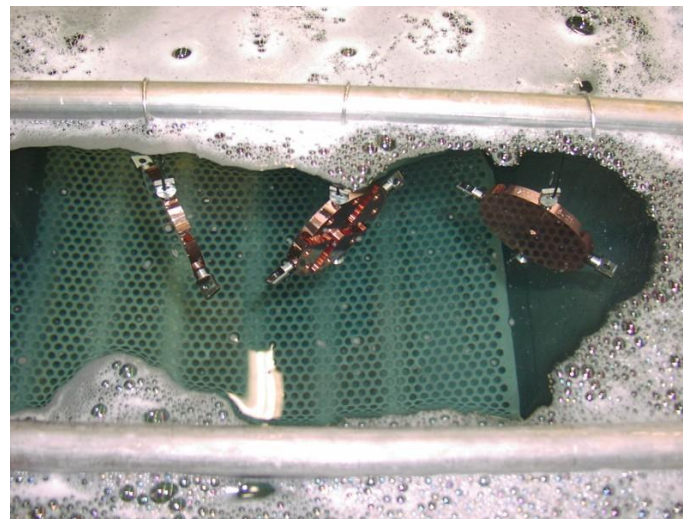
| Drawing no. | CLIAAS110337 Standard Cell Disk 21 |         |        |         |         |           | Prod. Nr. |      |
|-------------|------------------------------------|---------|--------|---------|---------|-----------|-----------|------|
| Description | 11 WDSDVGI.8KEK Standard cell      |         |        |         |         |           |           |      |
| Dimensions  |                                    |         |        |         |         |           |           |      |
| Measurand   | Description                        | Nominal | Upper  | Lower   | Actual  | Deviation | Pass      | Fail |
| 1           | Ref A [0.002]                      | 0.0000  | 0.0020 | 0.0000  | 0.0011  | 0.0011    | ✓         | ✓    |
| 2           | Outer diameter Ref B               | 74.0000 | 0.0025 | -0.0025 | 74.0015 | 0.0015    | ✓         | ✓    |
| 3           | [0.002]                            | 0.0000  | 0.0020 | 0.0000  | 0.0009  | 0.0009    | ✓         | ✓    |
| 4           | [0.002] A                          | 0.0000  | 0.0020 | 0.0000  | 0.0006  | 0.0006    | ✓         | ✓    |
| 5           | ø 70                               | 70.0000 | 0.0000 | -0.0100 | 69.9957 | -0.0043   | ✓         | ✓    |
| 6           | ø 70 [0.005] B                     | 0.0000  | 0.0050 | 0.0000  | 0.0010  | 0.0010    | ✓         | ✓    |
| 7           | Diameter 2xa                       | 5.1901  | 0.0025 | -0.0025 | 5.1900  | -0.0001   | ✓         | ✓    |
| 8           | Distance d                         | 8.7327  | 0.0020 | -0.0020 | 8.7334  | 0.0007    | ✓         | ✓    |
| 9           | Plane at distance d [0.002]        | 0.0000  | 0.0020 | 0.0000  | 0.0020  | 0.0020    | ✓         | ✓    |
| 10          | ø 70                               | 70.0000 | 0.0150 | 0.0100  | 70.0133 | 0.0133    | ✓         | ✓    |
| 11          | ø 70 [0.005] B                     | 0.0000  | 0.0050 | 0.0000  | 0.0007  | 0.0007    | ✓         | ✓    |
| 12          | Distance t                         | 1.1569  | 0.0025 | -0.0025 | 1.1562  | -0.0007   | ✓         | ✓    |
| 13          | Distance g                         | 7.5758  | 0.0025 | -0.0025 | 7.5765  | 0.0007    | ✓         | ✓    |
| 14          | Width Cross Z+                     | 11.8113 | 0.0025 | -0.0025 | 11.8131 | 0.0019    | ✓         | ✓    |
| 15          | Y-value symmetry Cross Z+          | 0.0000  | 0.0025 | -0.0025 | 0.0002  | 0.0002    | ✓         | ✓    |
| 16          | Width Cross Z-                     | 11.8113 | 0.0025 | -0.0025 | 11.8134 | 0.0022    | ✓         | ✓    |
| 17          | Y-value symmetry Cross Z-          | 0.0000  | 0.0025 | -0.0025 | 0.0002  | 0.0002    | ✓         | ✓    |
| 18          | Width Cross Y-                     | 11.8113 | 0.0025 | -0.0025 | 11.8122 | 0.0009    | ✓         | ✓    |
| 19          | Y-value symmetry Cross Y-          | 0.0000  | 0.0025 | -0.0025 | 0.0012  | 0.0011    | ✓         | ✓    |
| 20          | Width Cross Y+                     | 11.8113 | 0.0025 | -0.0025 | 11.8120 | 0.0007    | ✓         | ✓    |
| 21          | Y-value symmetry Cross Y+          | 0.0000  | 0.0025 | -0.0025 | 0.0003  | 0.0003    | ✓         | ✓    |
| 22          | Distance t                         | 1.1569  | 0.0025 | -0.0025 | 1.1563  | -0.0006   | ✓         | ✓    |
| 23          | Bottom plane cross [0.002]         | 0.0000  | 0.0050 | 0.0000  | 0.0005  | 0.0005    | ✓         | ✓    |
| 24          | Bottom plane cross [0.005] A       | 0.0000  | 0.0025 | -0.0025 | 0.0014  | 0.0014    | ✓         | ✓    |
| 25          | Iris [0.005] A B                   | 0.0000  | 0.0050 | 0.0000  | 0.0026  | 0.0026    | ✓         | ✓    |
| 26          | Cross [0.005] A B                  | 0.0000  | 0.0050 | 0.0000  | 0.0027  | 0.0027    | ✓         | ✓    |



**A. Degreasing with solvents Topklean MC 20A and Promosolv 71IPA**



**B. Degreasing with detergent NGL 17.40 spec. ALU III and ultrasound**



**C. Etching - Concentration :**

- phosphoric acid 70 %
- nitric acid 23.3 %
- acetic glacial acid 6.6 %
- hydrochloric acid 0.49 %



**D. Final rinsing with demineralised water and ultrasound, followed by rinsing with ethylic alcohol and ultrasound**

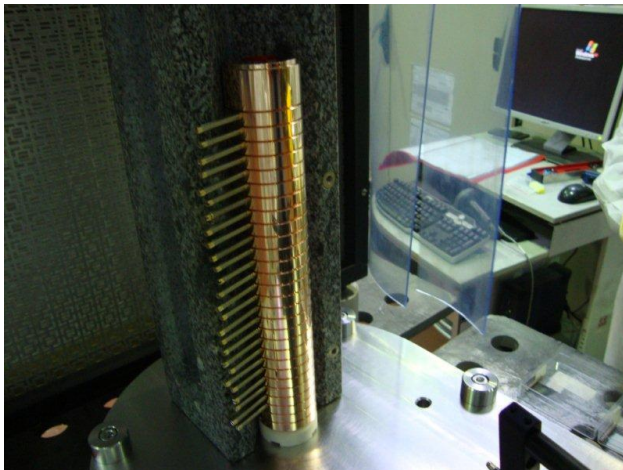
**E. Drying and packaging**



## Individual inspection



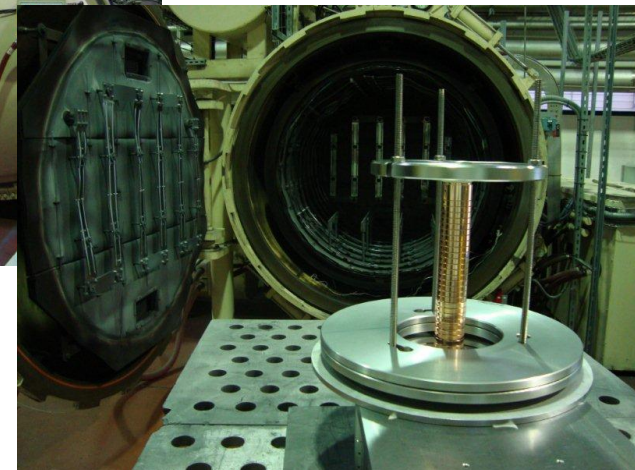
## Operation done under laminar flow



- Reference on the external diameter:
  - tolerance on external diameter:  $\pm 2 \mu\text{m}$
  - tolerance on the ref. line :  $\pm 2 \mu\text{m}$
- Alignment on a V-shape vertical support in granite (accuracy of  $\pm 1 \mu\text{m}$ )
- Straightness measurements before and after diffusion bonding cycle



## Ready for bonding





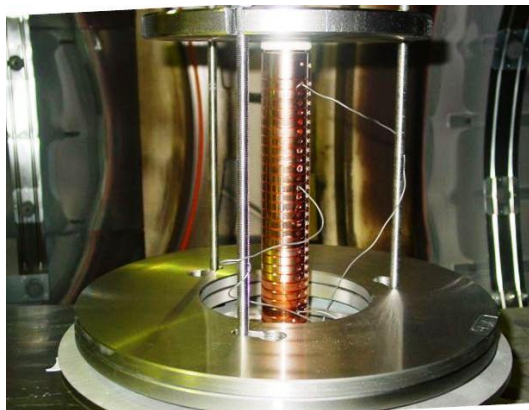


# DIFFUSION BONDING PARAMETERS AND HEAT CYCLE

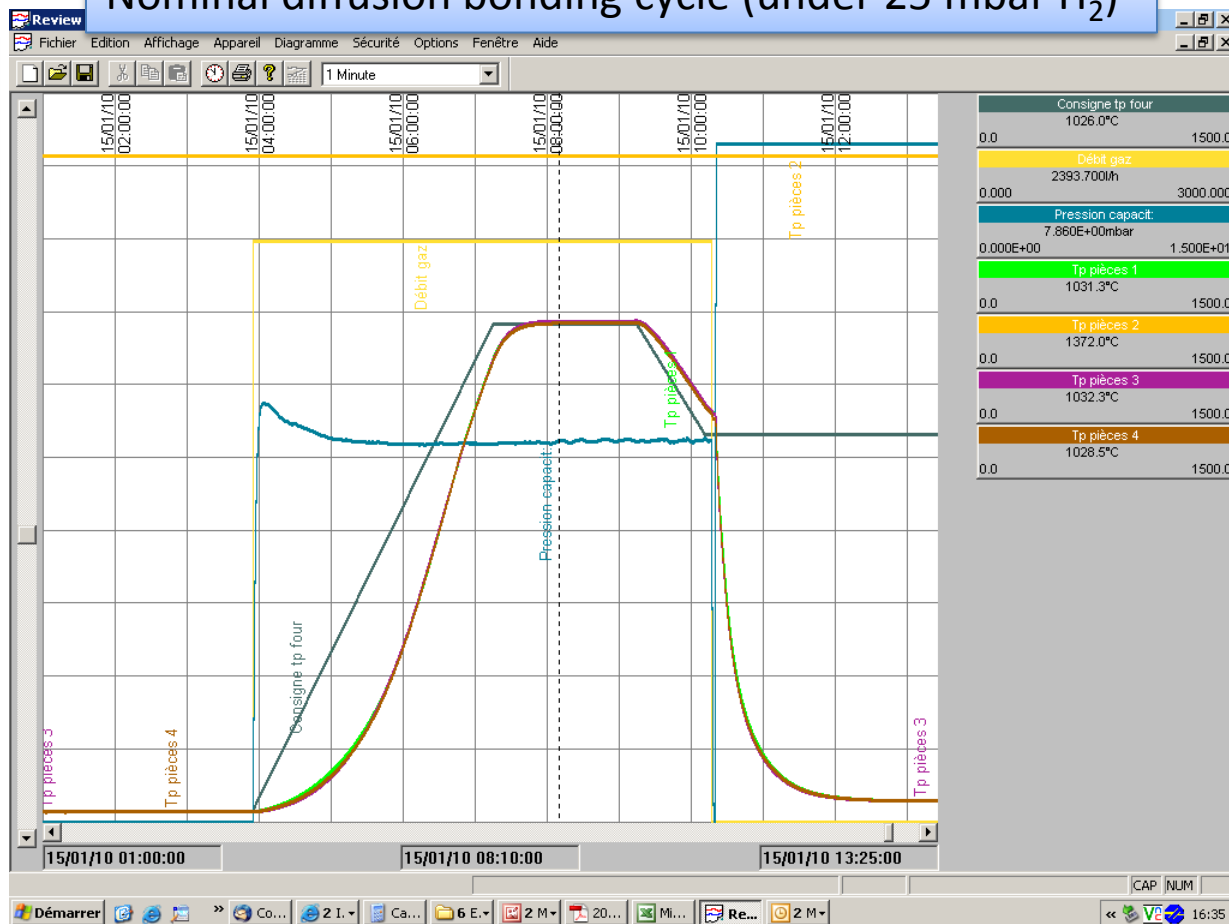
germana.riddone@cern.ch

Temperature: up to 1040°C  
Pressure: 0.28 MPa  
Holding time: 2 h

New infrastructure to  
guarantee uniform load

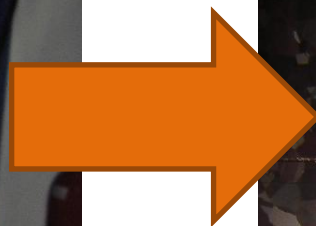
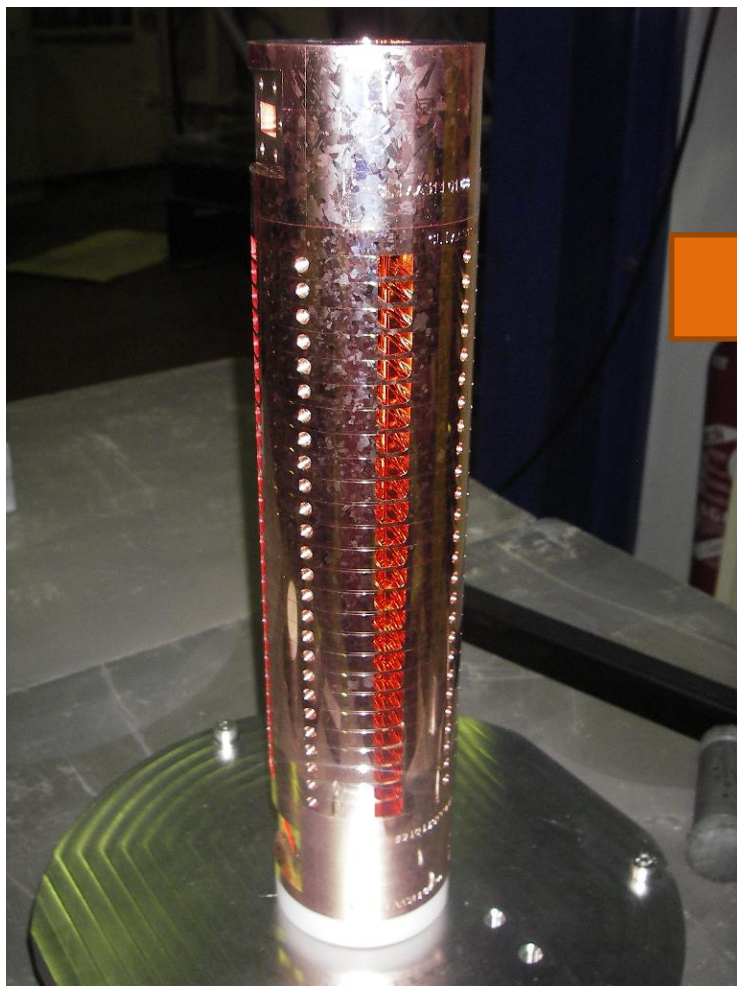


## Nominal diffusion bonding cycle (under 25 mbar H<sub>2</sub>)



Straightness measurement after diffusion bonding:  
variations within  $\pm 1.5 \mu\text{m}$









# CLEAN ROOM FOR ASSEMBLY AND MEASUREMENTS

germana.riddone@cern.ch

